Optimal design of hybrid distillation-membrane processes based on a superstructure approach

Dian Ning Chia[a], *Eva Sorensen*[a],[*]

[a] *Department of Chemical Engineering, University College London, Torrington Place, London WC1E 7JE, United Kingdom*

ABSTRACT

Considerable effort is currently being put towards process intensification to design more sustainable and energy-efficient processes. Hybrid distillation-membrane processes are prime examples of such intensified processes. In this work, different strategies are presented for how to handle the complexity of the membrane network of the hybrid process in terms of initialisation and convergence for simulation and optimisation. A superstructure approach for optimisation of membrane networks within hybrid processes is presented and verified. The energy consumption and economic performance of a hybrid distillation-pervaporation process, as well as that of the corresponding extractive distillation process, to separate a minimum-boiling azeotropic mixture are compared for different feed compositions. The impact of membrane properties and cost is also briefly considered. The results show that the total heat duty for the hybrid process is always lower than that of the extractive process for the system considered, confirming that the hybrid process is more energy efficient. In terms of total annualised cost, however, the hybrid process is found to be more economically attractive at lower feed compositions, while the extractive process is preferred for higher compositions.

1. Introduction

As part of the quest over the past few decades towards a more sustainable and energy efficient process industry, tremendous effort has been put towards process intensification (PI). A prime example of intensification is hybrid separation, often between a distillation column and a membrane process, where the advantages of one process is exploited to counteract the disadvantages of the other. A hybrid distillation/membrane process is for instance capable of separating azeotropic mixtures which cannot be separated by using only conventional distillation columns. Although membrane separations are capable of overcoming the thermodynamic restrictions imposed by azeotropes, when a high throughput and a high purity is required, which is typical in the chemical industry, a stand alone membrane separation will not be economically viable as it will require a large membrane area which is expensive (Skiborowski et al., 2013). An azeotropic mixture is typically separated by the use of an entrainer in an extractive distillation column, but the extractive process is both energy intensive and expensive due to the need for an additional column for entrainer recovery. Hybrid distillation/membrane processes have been found to save energy (Lipnizki et al., 1999), but may be limited by low capacity and high capital cost of the membrane unit, hence may not always be the best approach.

Due to the highly integrated and complex design of a hybrid distillation-membrane process (denoted just as a hybrid process in this work unless otherwise stated), the optimisation of the process is very challenging. Tula et al. (2020) discussed extensively the approaches that can be taken to solving model-based PI problems, such as the rule-based approach, direct solution approach (also known as superstructure optimisation), and hybrid solution approach.

However, this work will focus only on the superstructure optimisation approach. Previous work mostly simplifies the membrane network by considering only the membrane area, and/or a very limited number (typically up to three) of membrane stages in series. There has been little focus on the mathematical or numerical difficulties imposed by the membrane network in optimisation of hybrid processes, caused by the discrete, or integer, variables involved. Also, most studies considering the economic feasibility of hybrid processes have focused on only a specific feed composition, thus there is a lack of understanding of the effect of the feed composition on the performance of hybrid processes. Thus, in this work, a hybrid distillation-pervaporation process for ethanol/water separation is compared with a conventional extractive distillation process for the same separation for a range of feed compositions, with the objective of minimising the total annualised cost (TAC). Issues related to the optimisation of hybrid separation processes will also be discussed.

1.1. *Investigations of membrane networks*

Previous authors have found that the inclusion of a membrane unit with a distillation unit can improve the energy efficiency of the overall separation process (Lipnizki et al., 1999; Holtbrugge, 2016). The most commonly considered membrane processes for this are pervaporation (PV) and vapour permeation (VP). The key difference between these is the phase of their feed, where the feed in pervaporation is in the liquid phase while the feed in vapour permeation is in the gaseous phase (Vane, 2013). A membrane can also be categorised by module configuration, e.g., plate-and-frame, spiral wound, or hollow fibre module (Purkait and Singh, 2018). Although different membrane processes and module configurations may require different units and materials, their key working principles are similar, and a general membrane network model may therefore be applicable to most, if not all, cases for initial design studies.

Optimisation of membrane networks has been considered for several decades. In earlier days, the membrane networks considered were rather simple. Fan et al. (1968) considered a simple reverse osmosis network (RON) where the retentate of each membrane stage acted as the feed to the next membrane stage and the permeate was collected at each membrane stage. In their work, a portion of the retentate stream of a membrane stage could be recycled back to the feed of that membrane stage, and the split fraction (i.e., portion) of the retentate stream was therefore an optimisation variable. Evangelista (1989) proposed a variation of the structure proposed by Fan et al. (1968), and Kimura et al. (1969) proposed a structure which was adapted from the concept of a distillation column. El-Halwagi (1992) represented these structures using a state-space approach so that the different configurations of the RON could be considered in a *superstructure*. A superstructure of a chemical process is a representation that encompasses all process alternatives within a single mathematical model such that, when optimised, the optimal process design is determined alongside all the corresponding design and operating variables.

Up until then, the "smallest" building block for the membrane network was a complete unit (e.g., a membrane, a pump). Uppaluri et al. (2004) focused on the membrane unit (in particular a vapour permeation membrane) and split the

membrane unit into two sections, one for high pressure (i.e., retentate side) and another for low pressure (i.e., permeate side). In each section, there were n_c number of compartments, and in each compartment there were n_{sc} number of sub-compartments. A complete membrane was thereby made up of a pair of compartments (one in each section) that was again made up of n_{sc} number of sub-compartments. A mass-transfer relationship was considered between each pair of sub-compartments to simulate the membrane flux. The authors claimed that their superstructure could handle not only all possible configurations (including the number of membrane stages connected in series and the number of membrane modules connected in parallel) for the membrane units, as well as the membrane flow patterns (i.e., co-current, counter-current, and cross-flow patterns). However, their membrane network superstructure required many optimisation variables, which limited the upper bound of the membrane stages in the design that could be considered. Although the number of optimisation variables was not indicated in the paper, all case studies in their work consider only three membrane stages as the upper bound. Demirel et al. (2021) modified the superstructure of Uppaluri et al. (2004) by representing the membranes as generic building blocks (Demirel et al., 2017), which allowed the superstructure to capture the different membrane processes further (e.g., reverse osmosis, pervaporation, membrane absorption/stripping, and membrane with concentric layers). In the work by Demirel et al. (2021), for a membrane with three membrane stages and 10 sub-compartments in each membrane stage, there were 2683 variables, 4443 constraints, and 14864 non-zero elements. The size of the optimisation problem will increase significantly with the increasing number of membrane stages.

Instead of using a single unit as a building block, Kookos (2002) proposed a superstructure where the building block was made up of another, inner, superstructure module. The basic building block of the inner superstructure module was a single-stage membrane permeator consisting of a membrane with a feed, a permeate, and a retentate. Two or more single-stage permeators could be connected to form a continuous membrane column, and the inner superstructure module could then be formed by considering all the interconnecting streams between individual single-stage permeators and continuous membrane columns. The final, outer, superstructure was then formed by connecting several of these blocks together. Although the author claimed that all possible configurations could be modelled by this approach, a detailed mathematical description was not provided. Furthermore, the connections between non-adjacent single-stage permeators was also not considered. From their case studies, the number of single-stage permeators in the outer superstructure was not optimised, thus the difficulties and challenges of implementing the proposed superstructure with a large number of permeators remains unclear.

All the work mentioned so far considered some, if not all, of the inter-connecting streams within a membrane network, which requires significant computational effort to solve, and limits the number of membrane stages that can practically be considered. For instance, considering optimisation of a 10 × 10 membrane structure (i.e., the maximum number of membrane stages connected in series is 10, and within each membrane stage, the maximum number of membrane modules connected in parallel is 10), then the

membrane network superstructure become either inefficient or impossible due to the very large number of optimisation/decision variables. Instead of using the full membrane superstructure, Marriott and Sorensen (2003b) proposed a simplified superstructure for the optimisation of larger membrane networks. Defining first a membrane *module* as an individual membrane unit, and a membrane *stage* as a collection of membrane modules that are connected in parallel, then the authors assumed that all the membrane modules within a membrane stage were identical, i.e., the feed into a membrane stage is equally distributed between all of the membrane modules, which from a practical point of view is entirely sensible. For a membrane stage with k number of membrane modules, this approach avoids the optimisation of $k-1$ variables for the feed distribution, and only the value of k needs to be optimised, thus greatly decreasing the computational burden, especially when a large number of membrane stages is involved (i.e., $n \times (k-1)$ fewer variables for a $n \times k$ membrane structure). Marriott and Sorensen (2003b) also neglected the recycling of retentate and permeate streams back to previous modules to simplify the superstructure further, although recycle streams back to previous membrane stages can easily be added if required.

Although the membrane superstructure proposed by Marriott and Sorensen (2003b) is simple compared with the other membrane superstructures that considered all of the inter-connecting streams, their superstructure is more suited for complex and highly interconnected processes such as hybrid distillation-membrane processes that usually require many membrane stages and membrane modules (Lelkes et al., 2000; González and Ortiz, 2002; Luyben, 2009; Santoso et al., 2012; Roth et al., 2013; Valentínyi and Mizsey, 2014; Micovic et al., 2014; Skiborowski et al., 2014; Andre et al., 2018; Chia and Sorensen, 2022). Whilst being an efficient membrane network superstructure, Marriott and Sorensen (2003b) still performed their optimisations by repeated optimisation for fixed membrane stages, i.e., the number of membrane stages was not optimised simultaneously together with the other variables. This work will therefore use the superstructure proposed by Marriott and Sorensen (2003b), but will also allow for simultaneous optimisation of the number of membrane stages within the superstructure.

The superstructure optimisation problem of a distillation column is already complex due to the large number of discrete variables involved (e.g., the total number of stages, feed location, side draw location), and the complexity increased even more for a hybrid distillation-membrane process which involves a membrane network (e.g., number of membranes in series and parallel), thus a simplified membrane network such as the one proposed by Marriott and Sorensen (2003b) is typically used (Szitkai et al., 2002; Naidu and Malik, 2011; Koch et al., 2013; Skiborowski et al., 2014). One of the main challenges for the optimisation of this hybrid process is to optimise the membrane structure (i.e., simultaneously optimise the number of membranes in series and parallel). Binary variables are commonly used to determine the existence of a membrane in the membrane network, but it will lead to structural multiplicity (e.g., the pairs (0,1) and (1,0) for two membranes in a membrane network are actually the same structure, where only one membrane is actually present). Szitkai et al. (2002) proposed the "successive refinement" method to decrease the number of binary variables needed while optimising a membrane network. In the

method, the number of membrane modules, m, is represented as binary digits (e.g., (1,0) represents 2 and (1,1,1) represents 7), so now the cases (0,1) and (1,0) represent $m=1$ and $m=2$, respectively, thus eliminating structural multiplicity. The first step of the successive refinement approach is to consider the membrane modules with a coarser (i.e., larger) area so that a sub-optimal number of membrane modules can be approximated. Then, in the second refinement step, the membrane module areas for the membrane modules in question (e.g., if the sub-optimal number of membrane modules is four then membrane modules four and five are in question) will be refined to a smaller membrane area so that the optimal membrane area can finally be identified. The refinement step is repeated by refining the membrane module area until the smallest possible membrane module area is achieved. The successive refinement approach using binary digits may require extra constraints if the required lower or upper bounds of the number of membranes modules or stages are not $2^n - 1$ where n is the number of binary digits the user chooses (e.g., the maximum number of membrane modules that can be considered for three binary digits is $2^3 - 1 = 7 = 2^0 + 2^1 + 2^2$). The successive refinement method requires at least two optimisations (the first trial and the second refinement steps) and the actual number of steps (i.e., the number of optimisation required) should be determined by the user according to the complexity of the problem. Other than that, the final design of the membrane network is limited to a specific pattern where all membrane stages have the same number of membrane modules except for the last membrane stage. This may lead to sub-optimal designs as highlighted by (González and Ortiz, 2002; Skiborowski et al., 2014) and by this work which indicate that the optimal designs may have different membrane modules in different membrane stages. Naidu and Malik (2011) used a binary variable to indicate the existence of a membrane unit (e.g., 1 if it exists), which causes structural multiplicity. Skiborowski et al. (2014) introduced a bypass stream for each membrane stage and associated a binary variable to the bypass stream instead of to the membrane stage. When the bypass stream for membrane stage n is activated (i.e., the binary variable is 1 for bypass stream n), the feed of the membrane n will be directly sent to the retentate of membrane module n (i.e., the feed of membrane module $n+1$), thus voiding the existence of membrane module n. The structural multiplicity is limited by introducing an extra constraint to the optimisation problem.

Although a number of authors have considered the definition of a membrane network superstructure, and have to some extent considered its optimisation, there is still a lack of consideration of the difficulties faced when optimising such superstructures. Thus, one of the aims of this work is to discuss different strategies that can be applied to overcome the inevitable mathematical/numerical issues faced during the initialisation and/or convergence of the optimisation. In the following, we will propose and discuss different strategies that can be applied during the modelling and optimisation of the membrane network superstructure to overcome many of these issues (see Section 2). We will then compare and validate the performance of membrane network superstructure optimisation using the proposed strategy compared to the conventionally used repeated optimisation procedure with fixed number of membrane stages (see discussion in Section 3).

1.2. Investigations of hybrid distillation-pervaporation processes

The first mention of a hybrid distillation-pervaporation (D-PV) process was in a patent by Binning and James in 1958 for the dehydration of an isopropanol-ethanol mixture (Lipnizki et al., 1999). It was not until nearly 20 years later, however, that the process received attention in industry and began to be applied for the separation of various mixtures due to its capability to separate almost all kinds of liquid mixtures of various concentrations (Lipnizki et al., 1999), although are now more commonly used to separate azeotropic or close-boiling mixtures.

Van Hoof et al. (2004) presented a comparison between azeotropic distillation, the D-PV process, and a D-PV-D process (distillation followed by pervaporation and then followed by distillation again) for the dehydration of isopropanol. The simulation was carried out in Aspen Plus V11.1, and the design specification function in Aspen Plus was used to obtain the optimal distillation column design for each process. It is unclear, however, if the designs of the membrane unit(s) were decided a priori or if they were optimised. Moreover, from the final designs, it seemed that the authors did not perform a complete optimisation on the entire process as the column design (total number of stages, feed location, and reflux ratio) for the first column in all the processes are the same. Nevertheless, it was concluded that the D-PV process was the best process as it had significant energy cost savings (up to 48%) and it could save about 49% of the total cost (sum of the operating, capital, and maintenance costs).

Tula et al. (2017) compared the D-PV process with conventional distillation for separating alkanes and producing tert-amyl methyl ether using a shortcut method based on a driving force diagram. It should be noted that the authors considered only the energy savings of the distillation columns and not the overall costs. In each of the D-PV processes considered, there was only one membrane unit, although the membrane area was calculated based on the separation required. The results showed that the D-PV process could save energy for all the cases studied. Tgarguifa et al. (2018) also found that a 64% reduction in the operating cost and energy could be achieved by replacing the rectifying column of an industrial bioethanol purification process with a series of pervaporation membrane units. However, it is unclear how the operating and design parameters (including the number of membrane stages) were obtained, thus decreasing the reliability of the conclusions made. Furthermore, Lee et al. (2016) and Zarca et al. (2018) also studied the economic feasibility of a hybrid process under different membrane costs compared with the corresponding conventional distillation. Both studies showed that the hybrid process would become unfavourable with an increase in the membrane cost. Other than the standard D-PV processes, some researchers have also conducted investigations of other advanced hybrid processes such as coupling pervaporation with reactive distillation (Wang et al., 2019; Li et al., 2020) or with extractive distillation (Wu et al., 2020), which also showed great economic benefits by applying pervaporation within a hybrid process as compared to conventional separation.

Many studies of hybrid D-PV processes have shown that a pervaporation membrane unit can be coupled with different distillation configurations to improve the overall economic performance. However, the hybrid process may not always be superior to conventional distillation under different conditions, e.g., different membrane costs. In addition to the impact of membrane cost, there is also a lack of investigations comparing the hybrid process with conventional distillation for different feed compositions. Another aim of this work is therefore to show the overall performance of a hybrid process compared to conventional distillation based on extractive distillation for a range of feed compositions, as well as to consider the effects of membrane cost and the maximum allowable temperature of the membrane unit. These comparisons (detailed discussion in Section 3) can provide a more holistic view of the relative performance of the hybrid process vs conventional extractive distillation, and can identify when a hybrid process may be favourable, and when not.

2. Methodology

In this section, the proposed membrane network; the optimisation strategies for the membrane network; and the simulation and optimisation strategies of the hybrid process are described in detail. At the end of Section 2.2, the comparison between the three optimisation strategies explained in this work and between the methods available in the literature for simultaneous membrane superstructure optimisation (Szitkai et al., 2002; Naidu and Malik, 2011; Skiborowski et al., 2014) will be discussed.

2.1. Simulation and optimisation of membrane networks

This section describes the structure of the membrane network that has been adopted in this work. There are two important concepts involved (see Fig. 1): .

1. **Membrane module**: A membrane *module* is a standard membrane unit. This is illustrated in Fig. 1 as the smaller box with a diagonal line.
2. **Membrane stage**: A membrane *stage* consists of a set of membrane modules connected in parallel. This is illustrated in Fig. 1 as the larger box enclosing several membrane modules.

The simplified membrane network in Fig. 1 was first introduced by Marriott and Sorensen (2003b). The network includes N_{ms} membrane stages connected in series, and within each membrane stage there are $N_{mm,n}$ membrane modules connected in parallel, where the subscript n denotes the nth membrane stage. The membrane network ignores recycling between membrane stages (e.g., retentate from membrane stage 2 cannot be recycled back to membrane stage 1) as the recycling between two membranes stages significantly increases the mathematical complexity, especially for the optimisation task, but with minor or even no improvements for the membrane system studied by Marriott and Sorensen (2003b). Another assumption is that the feed to the membrane modules connected in parallel within a membrane stage is distributed equally. Marriott and Sorensen (2003b) claimed that for the membrane system they investigated, not only are there no clear benefits from controlling the distribution fraction, but it will also significantly increase the computational burden and optimisation complexity as there will then be $N_{mm} - 1$ distribution fractions that need to be optimised for each stage. A heater is present prior to each membrane stage to perform any required (re)heating of the feed into that membrane stage. With this membrane
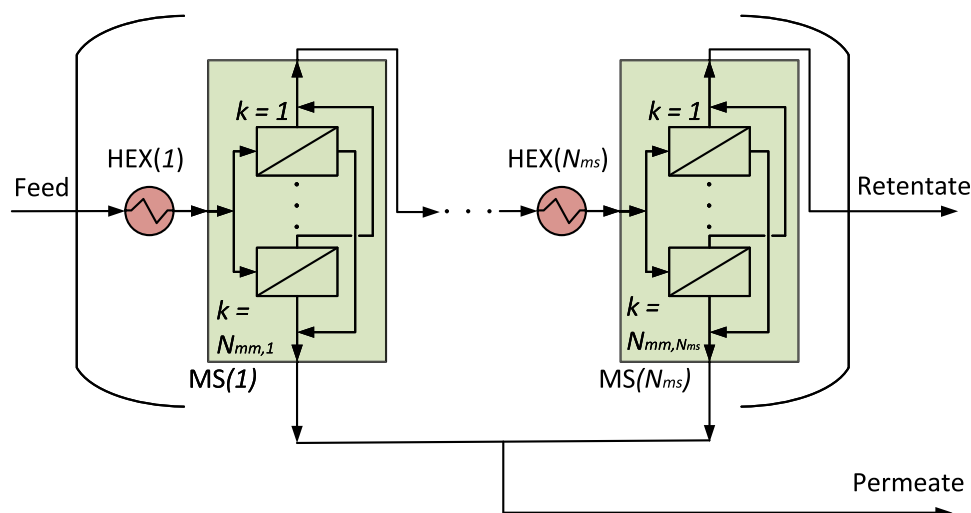
Fig. 1 – Schematic of the membrane network. The membrane stages (MS) are depicted with the larger boxes, while the membrane modules (MM) are the smaller boxes with a diagonal line enclosed within a membrane stage, and HEX(n) is the feed heater for membrane stage *n*. There are N_{ms} membrane stages in a membrane network, and there are $N_{mm,n}$ membrane modules in the nth membrane stage.

network, the total number of decision variables for a system with N_{ms} stages are:

$$N_{mv}^{tot} = 1 + 3 \times N_{ms} \qquad (1)$$

where the first term represents the decision of the number of membrane stages within the network and the second term represents the decisions of the number of membrane modules within each membrane stage (integer), as well as the existence (binary) and temperature (continuous) of each membrane stage feed heater.

2.2.   *Membrane system superstructure for simultaneous optimisation*

While there has been a number of studies over the years considering some form of optimisation of membrane networks, the literature rarely discusses the strategies adopted to overcome the initialisation and convergence difficulties faced during optimisation. Generally, the membrane superstructure is modelled as a composite model made up of N_{ms} membrane stages. Depending on the numerical solver used, the model will generally require N_{ms} to be a parameter, i.e., a constant value that cannot be varied during simulation or optimisation, and this may cause convergence difficulties when trying to find the optimal number of membrane stages, N_{ms}^{opt}. In this work, three strategies to overcome these numerical difficulties are introduced and discussed. In the following, the term "non-existing membrane" is defined as the membrane stages that are located *after* the N_{ms}^{opt} membrane stage. The strategies considered are illustrated in Fig. 2 (where only the stages and not the modules per stage are shown). The figure assumes that there are initially four membrane stages in the network, $N_{ms} = 4$, and that the optimal number of membrane stages is 2, $N_{ms}^{opt} = 2$. With the definition above, this means that *MS*(3) and *MS*(4) are redundant, or non-existing, membrane stages.

2.2.1.   *Strategy 1 – Zero flux*
The first strategy is the most straightforward option, where the non-existing membranes are eliminated either by directly setting the associated variables to zero or by using a binary variable

as a multiplication factor to the associated variables to indicate the non-existence. For example, as shown in Fig. 2a, the membrane permeate flux of the membrane modules in the non-existing membrane stages (*MS*(3) and *MS*(4)) can be set as zero (shown as the grey flux arrows), thus making these membrane stages redundant. Although the non-existing membrane stages are now redundant, the simulation results can still be obtained (although the flux etc. will be zero).

Despite being straightforward conceptually, this strategy is challenging to initialise and converge. A membrane model consists of differential equations, and the chances of successful initialisation and convergence are significantly increased with a good set of initial values. For a superstructure membrane network, there are many combinations (e.g., different combinations of numbers of membrane stages and modules), and it is impossible to provide a set of different initial values for each combination. Also, with this strategy, every single membrane module has the potential to have zero permeate flux, and will have this value for redundant membranes. However, this is difficult to implement during optimisation as additional "if-else" statements are required to model this, which further increases the complexity of the model as more discontinuities must be determined during simulation and/or optimisation. A strategy with zero flux may also cause problems as the existence of zeroes for these modules may cause not only numerical problems such as division by zero, but also causes a significant difference between the initial and final values which may be challenging numerically (i.e., many iterations may be required to converge the simulation successfully or the simulation may fail to converge).

2.2.2.   *Strategy 2 – Pseudo-feed*
To avoid the "zero" problems of Strategy 1, in this second option, the non-existing membrane stages are given feasible non-zero pseudo-feeds instead. Fig. 2b shows an example of feasible non-zero pseudo-feeds obtained by duplicating the feed into *MS*($N_{ms}^{opt} = 2$) (including all the stream information such as flow rate, composition, temperature, and pressure) and then using that feed information as the pseudo-feed into each of the non-existing membranes (shown in the figure as

(a) Strategy 1 – Zero flux

(b) Strategy 2 – Pseudo-feed
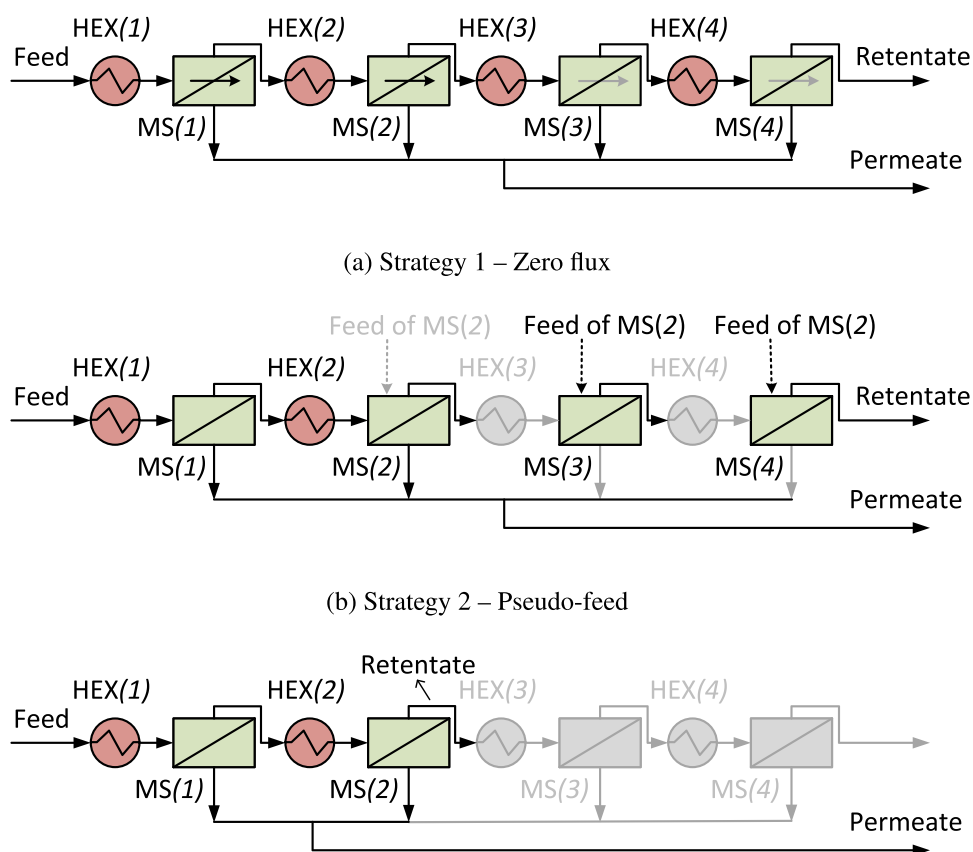
Fig. 2 – Schematics of the strategies proposed for the optimisation of the membrane system superstructure, illustrated for four membrane stages, $N_{ms} = 4$, and assuming that the optimal number of membrane stages is two, $N_{ms}^{opt} = 2$. (Only the membrane stages are shown in the figure).

the dotted lines on $MS(3)$ and $MS(4)$). The pseudo-feed for $MS(2)$ is greyed because it does not actually exist but is taken to be the retentate from the first membrane stage. All membrane stages except the first one will have a pseudo-feed into them. The first membrane stage does not require a pseudo-feed because it will always have an actual feed. In addition, the permeate streams from the non-existing membranes should not be added to the final permeate stream (shown as the grey permeate streams on $MS(3)$ and $MS(4)$). This can be done either by setting the permeate streams to zero or by removing the permeate streams as redundant streams. In this way, the membrane stages after N_{ms}^{opt} will become copies of the membrane at N_{ms}^{opt} (i.e., $MS(4) = MS(3) = MS(2)$), so the simulation results can still be obtained without difficulty. However, in order to utilise this strategy, a few additional "if-else" statements are still needed, which will cause discontinuities in the model and will increase the computational costs and difficulties similar to those discussed for Strategy 1.

2.2.3. Strategy 3 – Collect results at optimal membrane stage, $MS(N_{ms}^{opt})$

This final strategy is different from the other two strategies. It is assumed that separation takes place in all membrane stages regardless of the value of N_{ms}^{opt} (i.e., simulation continues in all membrane stages), but the results are collected at the optimal membrane stage, $MS(N_{ms}^{opt})$. The illustration of this strategy can be seen in Fig. 2c, where the results (permeate and retentate) are obtained at the optimal stage $MS(2)$ and the results for $MS(3)$

and $MS(4)$ are ignored. This strategy can effectively avoid the "zero" problems encountered in Strategy 1, and has fewer "if-else" statements compared to Strategy 2. Although not encountered in this work, theoretically, if the required product specification is high, the feed to the non-existing membrane stages may become "overly pure" and cause mass balance issues while solving the model. To minimise the chance of this issue, the number of membrane modules in the non-existing membrane stage can be set as one (i.e., $N_{mm,n} = 1$ where $n = [N_{ms}^{opt}, N_{ms}]$).

It should be noted that to reduce the number of optimisation variables (i.e., the number of binary optimisation variables) and also reduce the structural multiplicity, an integer is used to represent the actual (optimal) number of membrane stages (N_{ms}^{opt}) in the membrane structure. Two dummy arrays with the size of N_{ms} are created to hold the information about the elements of the actual permeate stream (*perm*) and the elements of the actual retentate stream (*ret*) as shown in Algorithm 1. Fig. 2c shows that the actual permeate stream is a collection of permeate streams obtained from the existing membrane stages (i.e., membrane stages up to N_{ms}^{opt}) and the retentate stream is collected from the retentate stream of only the optimal membrane stage (i.e., at membrane stage N_{ms}^{opt}), which is also reflected in Algorithm 1.

Algorithm 1. Collection of the elements needed for the actual permeate and retentate stream calculation using dummy arrays in Strategy 3 (the maximum number of membrane stages considered is N_{ms} and the optimal number of membrane stages is N_{ms}^{opt}).

```
for i ∈ [1, N_ms] do
    if i ≤ N_ms^opt then
        │ perm(i) = MS(i).permeate  // permeate obtained from membrane stage i
    else
        │ perm(i) = 0  // permeate is zero as membrane stage i does not exist
    if i == N_ms^opt then
        │ ret(i) = MS(i).retentate  // retentate obtained from membrane stage i
    else
        │ ret(i) = 0  // retentate is zero as membrane stage i is not the final optimal
        │   membrane stage
```

The actual permeate stream ($perm_{act}$) and retentate stream (ret_{act}) can be calculated using the corresponding arrays obtained in Algorithm 1:

$$perm_{act} = \sum_{i=1}^{N_{ms}} perm(i) \qquad (2)$$

$$ret_{act} = \sum_{i=1}^{N_{ms}} ret(i) = \max(ret) \qquad (3)$$

The other required information (e.g., the cost of the membrane stage feed heaters) could be obtained or calculated in a similar way.

2.2.4. Summary

In general, Strategy 1 is straightforward to implement as it only requires the flux of the non-existing membranes to be set to zero. However, the existence of zeroes may give rise to numerical issues, and the convergence may also be difficult due to the very different initial and final designs. Strategy 2, which uses non-zero pseudo feeds for the non-existing membrane stages, can avoid using zeroes, but this strategy requires the use of "if-else" statements that will increase the numerical difficulties. The final strategy, Strategy 3, proposes to allow the calculation to continue in all the membrane stages but to identify and collect only the results at the optimal membrane stage as the optimal solution. This strategy can avoid using zeroes, and it has fewer "if-else" statements compared to Strategy 2. As different systems may have different initialisation and convergence problems, there is no single criterion to quantify the performance of the strategies to allow a comparison. In our experience, however, the least initialisation and convergence difficulties are encountered when using Strategy 3 and this strategy is therefore recommended and used in this work. However, it should be noted that the "if-else" statements (see Algorithm 1) may limit the use of gradient-based optimisation, so a stochastic optimiser which does not rely on gradient information may be preferred when Strategy 3 is adopted. Only qualitative comparison can be provided because Strategies 1 and 2 often fail due to numerical problems. Similar observations are also reported by Szitkai et al. (2002) and Skiborowski et al. (2014) when binary variables are present.

Compared to the successive refinement method proposed by Szitkai et al. (2002), Strategy 3 requires only a single optimisation and allows a different number of membrane modules in each membrane stage. Compared to Naidu and Malik (2011), the avoidance of zeros (e.g., zero fluxes or feed in a non-existing membrane stage) increases the robustness of the model and optimisation, and a similar strategy is also applied by Skiborowski et al. (2014) through the introduction of bypass streams. However, the strategy by Skiborowski et al. (2014) requires the equation of the outlet stream of membrane stage n that is fed into membrane stage $n + 1$ (the retentate stream in this case) to be modified to include the influence of bypass stream (e.g., the retentate stream of stage n will not take the values of the retentate stream leaving membrane stage n but rather the values of the bypass which is the feed into membrane stage n). Strategy 3 proposed in this work does not require the membrane model equations to be modified, as only dummy arrays (see Algorithm 1) are introduced to collect and transform the stream information into the desired results. Moreover, unlike Naidu and Malik (2011) and Skiborowski et al. (2014), Strategy 3 does not involve binary variables to determine the existence of a membrane stage, instead, "if-else" statements are required to collect the final results. Since Strategy 3 only needs the information from each membrane stage without modification of any connecting equations, and the performance of all membrane stages was calculated, it can easily be applied to a membrane network acting as a black-box superstructure method.

2.3. Simulation and optimisation of hybrid processes

Fig. 3 shows the flowsheet of the hybrid distillation-pervaporation (D-PV) process studied in this work, where it has been assumed that the azeotrope in the feed is a minimum boiling azeotrope. The fresh feed is first fed into the distillation column, and a stream close to the azeotropic composition leaves the column in the distillate. If the distillate temperature is higher than the maximum allowable temperature of the membrane, then a distillate cooler is needed to cool the distillate down to the maximum temperature of the membrane. In this case, the existence of the membrane feed heater into the first membrane stage, $HEX(1)$, should be removed (i.e., the binary variable, $b_{HEX,1} = 0$). The distillate cooler can be removed if the distillate temperature is lower than the maximum allowable temperature, and the heater is then needed to increase the temperature up to the maximum temperature (the separation performance is best at high temperature). Since the membrane considered in this work is a pervaporation membrane, the distillate may need to be pressurised to ensure that the distillate remains in the liquid phase also after the first membrane stage feed heater. Then, the pressurised and heated (if required) distillate enters the membrane network. As the separation principle of the membrane does not depend on thermodynamic equilibrium, the azeotropic stream can be separated into its pure
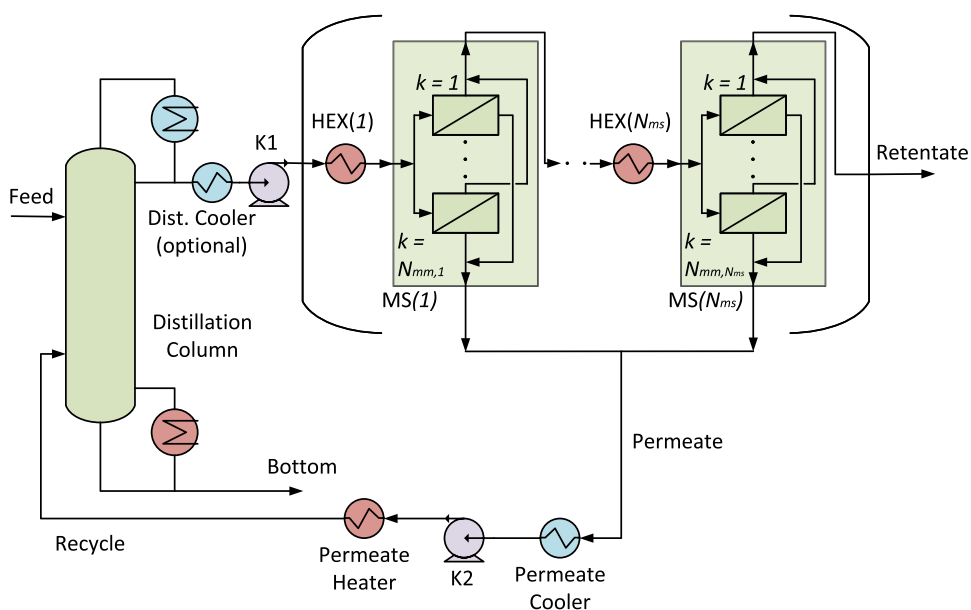
Fig. 3 – Flowsheet of the hybrid distillation-pervaporation process. The detailed membrane network is shown in Fig. 1.

components assuming a suitable membrane has been identified. (Membrane selection can of course also be included as part of the superstructure but has not been considered in this work.) The desired product is in this work assumed to be collected in the retentate, while the remaining component(s) leave the membrane network in the permeate and are either collected as product or more likely recycled back to the column for further processing. As the permeate is a low-pressure vapour, a permeate cooler is first used to cool the vapour to its saturated liquid phase at the permeate pressure (typically close to vacuum) before passing the low-pressure saturated liquid into a pump to increase the pressure up to the operating pressure of the distillation column. Since there is an increase in pressure, the liquid is now sub-cooled, hence a permeate heater is required to raise the temperature to its saturated liquid temperature before entering the distillation column. Depending on the mixture and the membrane used, the permeate may be pure enough to be directly collected as a product, i.e., the permeate does not need to be recycled back into the distillation column. In this case, the heater is not required as it is assumed that the product will then be directed to a product tank.

The D-PV process is initialised, simulated, and optimised using the procedure proposed in Fig. 4. First, a rough mass balance calculation around each unit (without considering the recycling stream) is carried out to initialise the model by assuming that the distillate is at the azeotropic point and all the product streams are at their required purities. Then, a suitable shortcut method (e.g., McCabe-Thiele method or driving force diagram method (Gani and Bek-Pedersen, 2000) can be used to obtain the initial design of the distillation column, again without considering the recycling stream. With this initial design, the column and the membrane network are then first simulated separately. The simulation results for the individual units are saved and then used as preset, or initial, values for the actual D-PV process, i.e., the distillation column and membrane unit together, coupled with the recycling stream. If the initial simulation of the D-PV process fails, then one or more of the key variables (e.g., number of distillation column stages, number of membrane stages/modules) in the individual units should be changed

and the process re-simulated. A good rule-of-thumb is that the initial designs of the individual units should give results that are relatively close to the product specification (e.g., $0.90\,mol\,mol^{-1}$ if the product specification is $0.99\,mol\,mol^{-1}$). Once the simulation of the D-PV process succeeds, the model can then be optimised with a suitable MINLP optimiser.

Regarding the MINLP optimiser, either deterministic optimisation (e.g., Outer Approximation/Equality Relaxation/Augmented Penalty), stochastic optimisation (e.g., Genetic Algorithm, Particle Swarm Optimisation, or Simulated Annealing), or combined stochastic-deterministic optimisation (e.g., Chia et al. (2021); Duanmu et al. (2022a)) can be applied. In our experience, stochastic optimisation or combined stochastic-deterministic optimisation is preferred due to their high robustness. Deterministic optimisation is very sensitive to the initial values of each optimisation variable, especially with the large number of integer optimisation variables in the hybrid process (e.g., the total number of stages and feed locations of a distillation column, and the number of membrane stages and of modules, as well as existence of membrane feed heaters). It should be noted that in this work the existence of membrane stage feed heaters is determined by the optimisation simultaneously with the rest of the design. Strictly speaking, the temperature of the membrane feed stage heaters should also be optimised, however, this will further increase the complexity of the optimisation problem due to the addition of n more variables. Bausa and Marquardt (2000) stated that the permeate flux through the membrane is higher at a higher temperature, i.e. the performance of the membrane is better for higher temperatures. Based on this statement, the membrane network can be further simplified by assuming that the output temperature of the membrane stage feed heaters can be fixed at the maximum allowable temperature of the membrane.

3. Optimal results

There are two main aims of this work: (1) to validate the membrane network superstructure, and (2) to compare the performance of the hybrid process relative to a conventional extractive distillation process. To illustrate the proposed
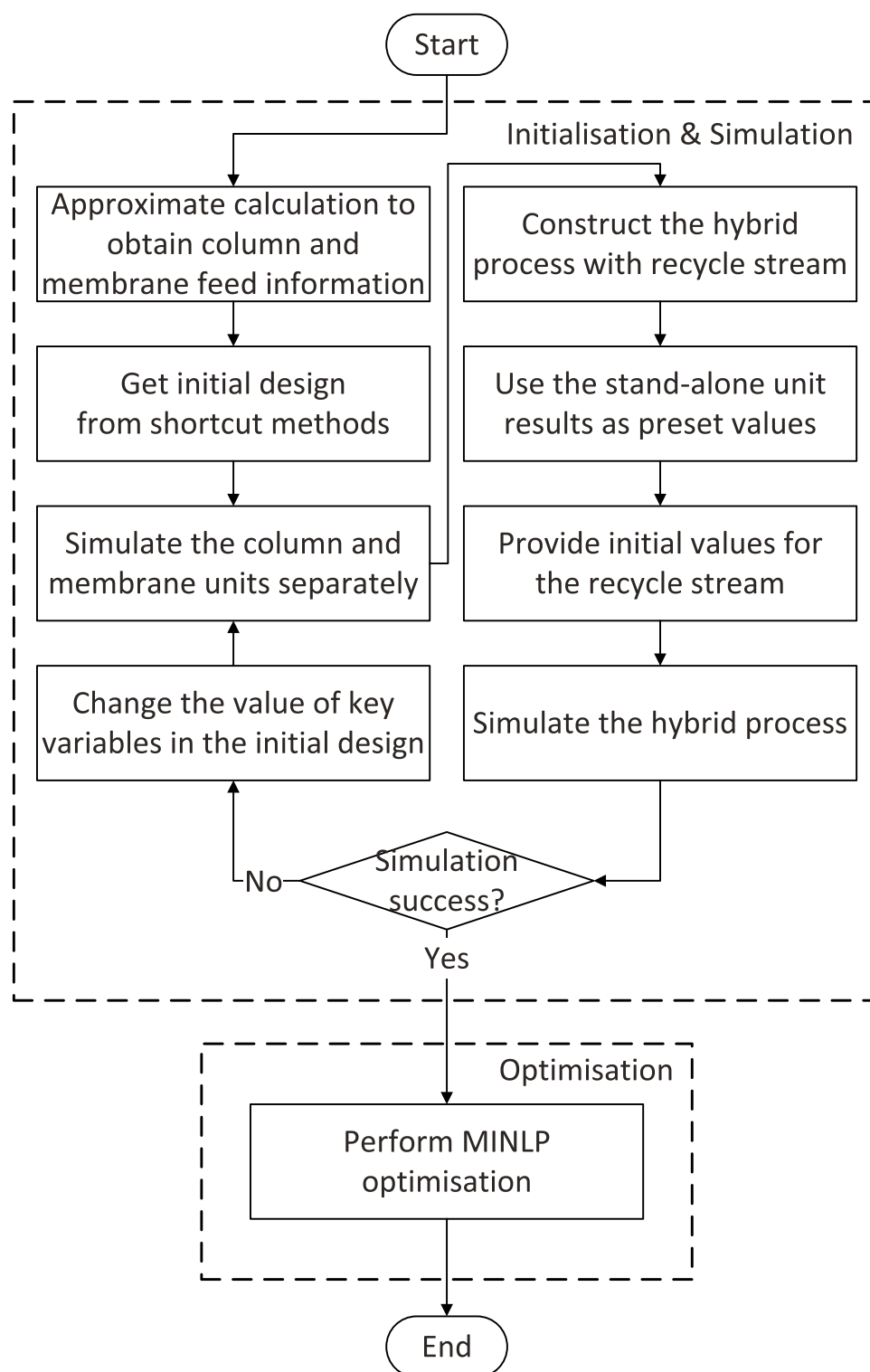
Fig. 4 – The initialisation, simulation, and optimisation procedure for the hybrid process.

procedure, we will consider the separation of an azeotropic ethanol/water mixture. All the simulations and optimisations are performed with gPROMS Process (Process Systems Enterprise, 2021). The physical properties of the liquid phase are described by the UNIQUAC model, while the physical properties of the vapour phase are described by the ideal gas model. The feed is considered to be 500 $kmol\,h^{-1}$ at 1 bar, and the feed composition varies according to the objective of the investigation, which will be detailed in the following subsections. The distillation columns, pumps, and heaters are

modelled with the built-in library models. The columns are assumed to be operating at 1 bar, i.e., without any pressure drop. Once the near azeotropic distillate leaves the distillation column, it is pressurised to 5 bar so that the distillate will not vaporise after being heated by the membrane feed heater (Luyben, 2009), while the permeate pressure is maintained at a very low pressure of 400 Pa (taken from the experimental setup by Tsuyumoto et al. (1997). The user-defined membrane model can be found in Appendix A, and the flux equations are taken from Tsuyumoto et al. (1997). The

maximum allowable temperature of the membrane is assumed to be the highest temperature investigated in Tsuyumoto et al. (1997), which is 70°C. Therefore, unless stated otherwise, the membrane feed heater (if it exists) will heat the membrane feed to 70°C. The selection of the heating and cooling source for different units is automated during simulation using "if-else" statements. The details of the available utility sources can be found in Table B1.

The optimisation task is to minimise the total annualised cost (TAC), where the sizing and costing equations for the distillation column can be found in Duanmu et al. (2022b), and the costing equations for the other units (membrane, pump, heater/cooler) can be found in Appendix B. At least 99 $mol\%$ ethanol and water product purities are required in the ethanol and water product streams, respectively. The optimisation variables include both discrete (total number of stages, feed location, recycle location, number of membrane stages connected in series, number of membrane modules connected in parallel, and the existence of heat exchangers) and continuous variables (reflux ratio, distillate/bottom flow rate, and makeup flow rate). It should be noted that the total number of stages and feed/recycle locations are each represented by a single integer value during optimisation. The number of optimisation variables associated with the membrane network is reported in Equation (1), but the number of optimisation variables is reduced to $1 + 2 \times N_{ms}$ because the membrane feed temperature is fixed. Therefore, in the case studies, the hybrid processes have a total of 26 optimisation variables, 21 optimisation variables associated with the membrane system for $N_{ms} = 10$ and 5 optimisation variables associated with the distillation column (total number of stages, feed location, recycle location, reflux ratio, and distillate flow rate). The extractive processes have a total of 10 optimisation variables, 6 optimisation variables in column C1 (total number of stages, feed location, recycle location, reflux ratio, distillate flow rate, and makeup flow rate) and 4 optimisation variables in column C2 (total number of stages, feed location, reflux ratio, and bottom/recovery flow rate). The key parameters for the membranes for each of the cases considered can be found in Table 1. The plant is assumed to be operating 8400 $h\,year^{-1}$, and the payback period is assumed to be 8 $years$ (Duanmu et al., 2022b).

The optimiser used in this work is a Genetic Algorithm (GA) coded externally to gPROMS in C#, where gO:RUN (Process Systems Enterprise, 2022) is used for the communication between the external optimiser and the gPROMS simulations. A dual Intel Xeon Gold 6226R CPU (32 cores and 64 processors in total) with a clock speed of 2.90 GHz and the RAM with a total memory capacity of 192 GB (3200 MHz) are used for optimisation. The main settings for the GA are a population size of five times the number of decision variables (130 populations for hybrid processes and 50 populations for extractive processes), an elite percentage of 10% (i.e., the top 10% of the population in the current generation will directly become the children of the next generation), tournament selection with four players to select the parents for the next generation, flat crossover method, and uniform mutation. There are two stopping criteria active for GA, which are (1) a maximum of 200 generations reached and (2) the best value of the objective function stays within a tolerance of 10^{-4} for 20 consecutive generations. GA will stop depending on which of the two stopping criteria is achieved first. 40 workers/processors are used in a master-slave parallel computing structure to speed up the optimisation process. The optimisation variables are considered as real and integer values in

Table 1 – Key membrane parameters, where the values in the base case taken from González and Ortiz (2002), for the hybrid distillation-pervaporation processes used in each case study.

| Parameter | Case Study | | | Unit |
	Base	Half Cost	90°C	
Membrane Price*	1063	531	1063	$ m^{-2}
Membrane Replacement*	200	100	200	$ $m^{-2}\,y^{-1}$
Membrane/Heater Temp.	70	70	90	°C
Membrane Lifetime	2			y

*Price in 2002, $CEPCI_{2002} = 396$

their original form without transformation into binary digits, i.e., the number of genes equal to the number of optimisation variables. The inequality constraints are handled using the penalty function proposed by Deb (2000), and GA treats all the variables equally (e.g., all variables have the same mutation probability in a generation). Due to the randomness associated with the stochastic optimiser, there is no guarantee for the global optimum and the results may also be a poor local optimum. Therefore, for each optimisation task, the optimisation is repeated multiple times (here at least five times) to ensure a good optimal solution has been found.

3.1. Validating the membrane network superstructure approach

To verify that this superstructure approach is indeed successful, we will compare our approach to the old approach of repeating the optimisation for each number of membrane stages. In the following, the feed composition will be fixed at 0.10 $mol\,mol^{-1}$ ethanol. The number of membrane stages is then fixed at 4–9 stages and optimisations are carried out for each fixed stage number (denoted "Repeated Optimisation" in Table 2). Then, the main optimisation is carried out using the superstructure proposed in this work (denoted "SS" in Table 2), where N_{ms}^{opt} is now an optimisation variable with a range of [4,9], i.e. the stage number is decided by the optimiser.

The main optimisation results are shown in Table 2. Due to space limitations, the existence of the heater before each membrane stage (optimised as a binary variable) is not shown. However, the optimisation results show that for each design, the first heater is not required but a cooler is required before the membrane system to cool down the distillate (the boiling point of the azeotropic mixture is 78°C) to the maximum allowable membrane temperature (70°C). Moreover, except for the design with nine membrane stages, where heaters on stages six and nine are absent, all other designs, including for the superstructure optimisation, require heaters before each of the membrane stages.

The best design found from the repeated optimisation is for seven stages, i.e. when $N_{ms} = 7$, with a TAC of $ 1.73 $M\,y^{-1}$. The superstructure optimisation also found that the hybrid process with seven membrane stages is the best design, with the same TAC. Considering the individual design variables (e.g., the total number of stages of the distillation column, distillate flow rate, reflux ratio, and membrane network modules per stage) for both designs, it is clear that the optimal designs are very similar. In terms of computational effort, the superstructure optimisation requires a single

Table 2 – Optimal results for the hybrid distillation-pervaporation process optimised with a fixed number of membrane stages (Repeated Optimisation) and with the number of membrane stages as a free optimisation variable in the superstructure (SS). The ethanol feed composition is fixed at 0.1 $mol\,mol^{-1}$.

Item	Repeated Optimisation $N_{ms}=4$	$N_{ms}=5$	$N_{ms}=6$	$N_{ms}=7$	$N_{ms}=8$	$N_{ms}=9$	SS	Units
Column C1								
Total stages	26	23	23	22	21	21	22	–
Feed stage	22	20	19	17	17	17	17	–
Recycle stage	25	22	22	21	20	19	21	–
Distillate	56.11	56.27	56.69	57.53	56.94	57.32	57.77	$kmol\,h^{-1}$
Reflux ratio	1.36	1.39	1.30	1.17	1.27	1.24	1.15	$mol\,mol^{-1}$
Reboiler duty	1521	1544	1498	1441	1486	1481	1437	kW
Condenser duty	− 1427	− 1450	− 1404	− 1348	− 1393	− 1387	− 1343	kW
Membrane Network*								
No. membrane stages	4	5	6	7	8	9	7	–
No. modules in stage 1	24	21	13	10	6	10	9	–
No. modules in stage 2	30	29	14	14	6	17	12	–
No. modules in stage 3	41	31	25	13	13	18	14	–
No. modules in stage 4	65	27	26	14	6	11	12	–
No. modules in stage 5	–	42	26	23	18	7	23	–
No. modules in stage 6	–	–	39	27	18	15	33	–
No. modules in stage 7	–	–	–	40	30	32	39	–
No. modules in stage 8	–	–	–	–	40	20	–	–
No. modules in stage 9	–	–	–	–	–	12	–	–
No. modules in stage 10	–	–	–	–	–	–	–	–
Total no. modules	160	150	143	141	137	142	142	–
Total membrane area	960	900	858	846	822	852	852	m^2
Membrane heating duty	121	128	134	147	139	144	149	kW
Distillate cooling duty	− 18	− 18	− 18	− 18	− 18	− 18	− 18	kW
Permeate cooling duty	− 134	− 136	− 141	− 153	− 147	− 149	− 156	kW
Permeate heating duty	23	23	24	26	25	25	27	kW
Total Duty								
Heating	1665	1696	1656	1614	1650	1650	1613	kW
Cooling	− 1579	− 1604	− 1563	− 1519	− 1557	− 1554	− 1517	kW
Capital Cost (CAPEX)								
Column	0.55	0.45	0.45	0.42	0.40	0.39	0.42	$M\,\$$
Membrane	5.26	4.93	4.70	4.64	4.51	4.67	4.67	$M\,\$$
Reboiler	0.36	0.36	0.35	0.34	0.35	0.35	0.34	$M\,\$$
Condenser	0.27	0.27	0.26	0.26	0.26	0.26	0.26	$M\,\$$
Others	0.88	1.01	1.14	1.28	1.40	1.28	1.28	$M\,\$$
Operating Cost (OPEX)								
Heating	0.71	0.72	0.70	0.69	0.70	0.70	0.69	$M\,\$\,y^{-1}$
Cooling	0.05	0.05	0.05	0.05	0.05	0.05	0.05	$M\,\$\,y^{-1}$
Electricity	Trace	Trace	Trace	Trace	Trace	Trace	Trace	$M\,\$\,y^{-1}$
Mem. Replacement	0.15	0.14	0.13	0.13	0.13	0.13	0.13	$M\,\$\,y^{-1}$
Overall								
CAPEX	7.31	7.03	6.91	6.93	6.92	6.95	6.96	$M\,\$$
Ann. CAPEX	0.91	0.88	0.86	0.87	0.86	0.87	0.87	$M\,\$\,y^{-1}$
OPEX	0.90	0.91	0.88	0.87	0.88	0.88	0.87	$M\,\$\,y^{-1}$
TAC	1.82	1.79	1.75	1.73	1.74	1.75	1.74	$M\,\$\,y^{-1}$
CPU time †	744	491	523	674	1037	509	690	s
Total CPU time	3978						690	s

* Existence of the membrane feed heater is also optimised. The heaters exist only between the second to membrane stage N_{ms} (for the repeated optimisation) or N_{ms}^{opt} for all designs, except for the design for $N_{ms}=9$ in repeated optimisation where the heater on stage six and nine are also absent. † Time needed for parallel computing with 40 workers/processors.

optimisation (CPU of 690 s for the complete optimisation), while with repeated optimisations, a total of 3978 s is required, which is about five times longer. Therefore, the proposed superstructure optimisation procedure can be seen to be both reliable and highly efficient.

A few additional observations can be made. Table 2 shows that a larger membrane system may benefit the design, for example, the TAC drops from \$ 1.82 M y^{-1} to \$ 1.73 M y^{-1} as the number of membrane stages increases from four stages to seven stages. It can also be seen that from six membrane stages and above, the TACs varies between \$ 1.73 M y^{-1} and \$ 1.75 M y^{-1}, i.e. the optimum is almost flat in terms of the stage number. This finding is also reported by Marriott and Sorensen (2003b). For these designs (from six to nine stages), the total number of membrane modules needed are also very similar (between 137 and 143 modules). It seems reasonable, however, that as shown here there will be a turning point (at seven membrane stages in this case) where the TAC will continue to increase after that point. Therefore, reliable optimisation is necessary to find the optimal design.
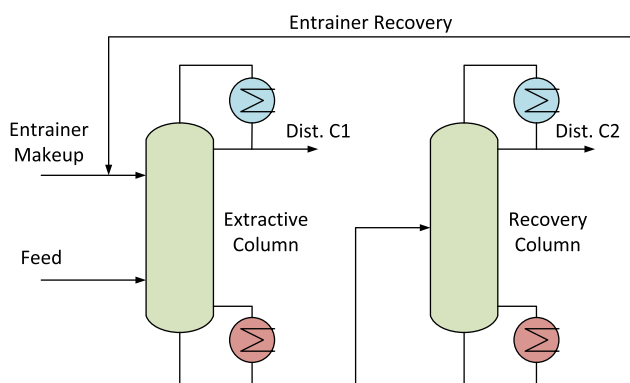
Fig. 5 – Flowsheet of the extractive distillation process.

3.2. Optimal design of an extractive distillation process

In the following, we will consider the extractive distillation process for the same separation as above, i.e. ethanol dehydration. The most common separation method to purify this mixture is extractive distillation (shown in Fig. 5) with ethylene glycol as the (heavy) entrainer (Li and Bai, 2012), thus this process is used as the base case to which we will compare the performance of the hybrid process. Therefore, let us first consider the optimal design of the extractive distillation process at different feed compositions with the optimal results tabulated in Table 3 and an example flowsheet
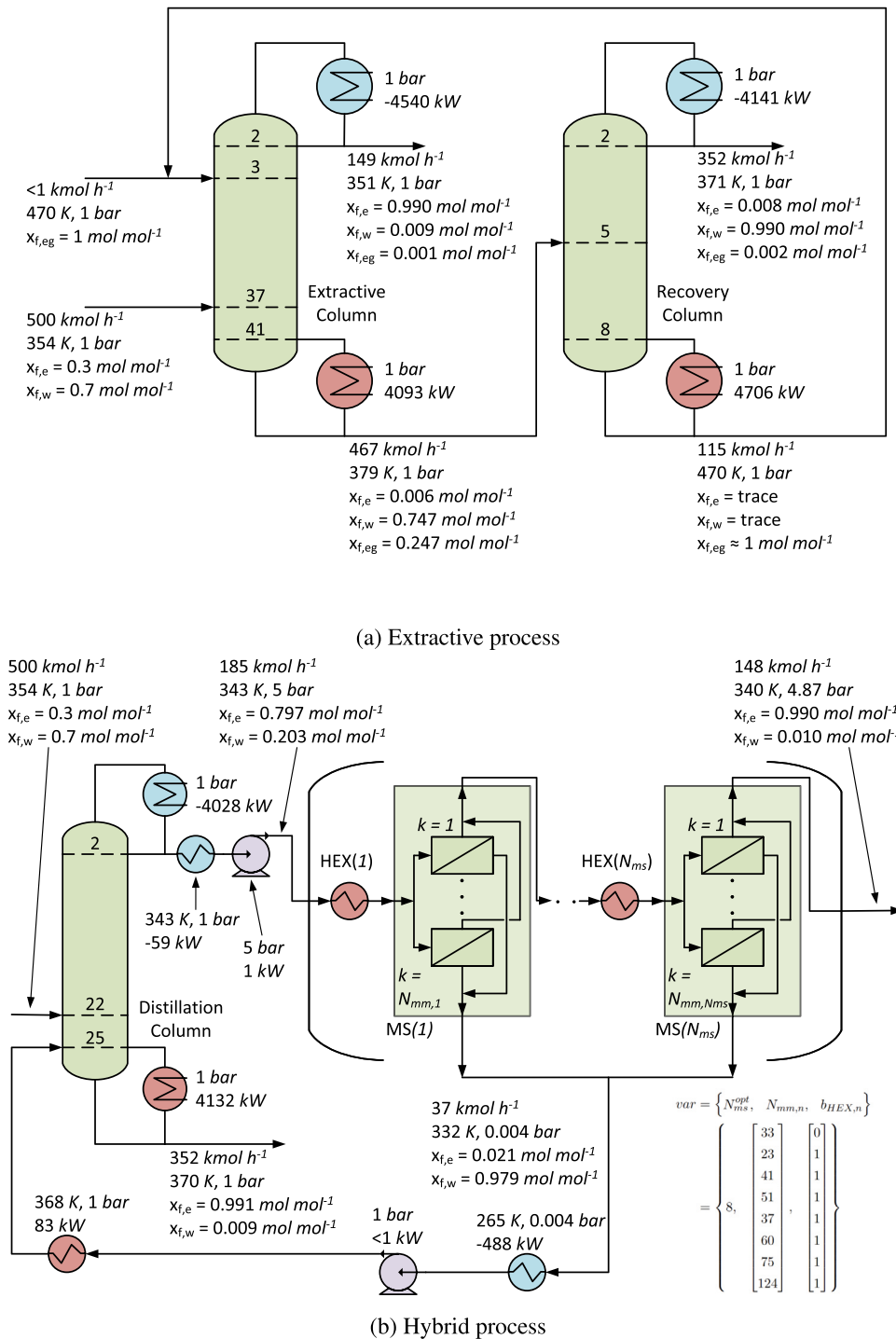
for the optimal structure of the extractive process at 0.30 molar composition of ethanol in the feed stream is shown in Fig. 6a. The upper bound for the feed composition is $0.80 \, mol \, mol^{-1}$ because the azeotropic point is at about $0.90 \, mol \, mol^{-1}$. From the table it can be observed that, in general, the total number of stages in column C1 (i.e., the extractive column) first increases then decreases, with a peak at $0.30 \, mol \, mol^{-1}$. This trend is expected and was also observed by Luyben (2005) for a conventional binary distillation. Taking the two end points as examples, at $0.10 \, mol \, mol^{-1}$ composition of either ethanol or water (i.e., both ends of the composition range considering that the azeotropic point is at $0.90 \, mol \, mol^{-1}$ ethanol), even without too much separation effort, the product streams are already relatively pure (i.e., near $0.90 \, mol \, mol^{-1}$ water composition at the bottom stream for low ethanol feed composition, or near the azeotropic point at the distillate stream for high ethanol feed composition). Therefore, as the feed composition moves away from the end points, the total number of stages must increase to purify the product streams, hence there will be a maximum between the two end points, which is exactly what is observed here.

The recycle stage of column C1, i.e., the feed stage for the entrainer stream from the recovery column, is always located near the top of the column, as expected, while the fresh feed stage is located near the bottom of the column (Li and Bai, 2012). As the feed composition increases, the amount of ethanol in the feed increases, thus the distillate

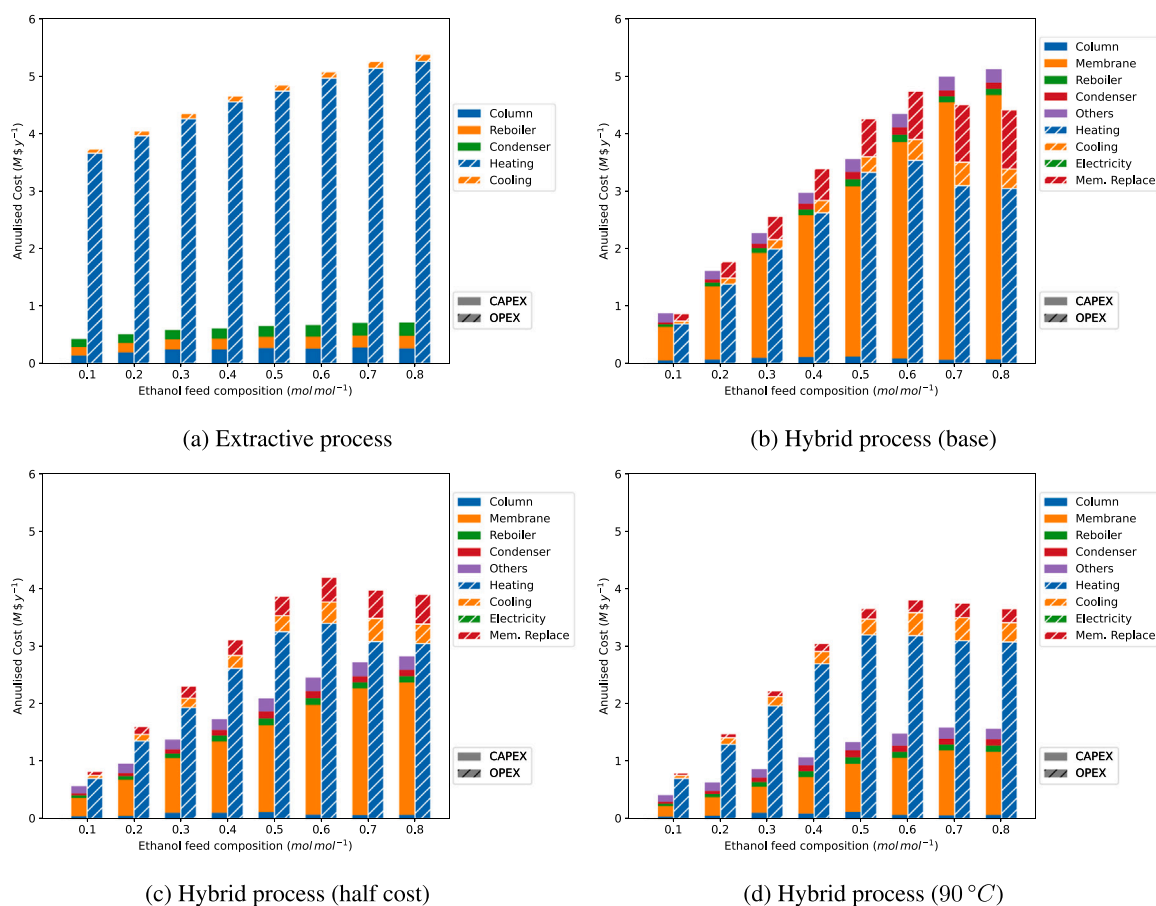|	Table 3 – Optimal results for the extractive distillation process at different ethanol feed compositions.								
	Ethanol Feed Molar Composition								
Item	0.10	0.20	0.30	0.40	0.50	0.60	0.70	0.80	Units
Column C1 (Extractive Column)									
Total stages	32	37	42	38	39	37	37	33	–
Feed stage	28	31	37	33	33	31	30	25	–
Recycle stage	3	3	3	3	3	3	3	4	–
Makeup flow rate	0.61	1.00	0.94	0.70	0.37	0.39	0.89	0.12	$kmol \, h^{-1}$
Distillate	46.49	98.02	148.84	199.68	250.35	301.38	353.03	403.34	$kmol \, h^{-1}$
Reflux ratio	2.82	2.10	1.88	1.77	1.62	1.55	1.47	1.39	$mol \, mol^{-1}$
Reboiler duty	1748	2911	4093	5189	6093	7154	8209	9163	kW
Condenser duty	− 1881	− 3222	− 4540	− 5853	− 6947	− 8145	− 9250	− 10,189	kW
Solvent-to-feed ratio	0.09	0.17	0.23	0.34	0.45	0.56	0.67	0.81	–
Column C2 (Recovery Column)									
Total stages	9	9	9	9	11	11	15	12	–
Feed stage	5	5	5	5	6	6	10	6	–
Recovery flow rate	42.73	83.88	114.59	168.84	223.81	280.24	332.98	403.67	$kmol \, h^{-1}$
Reflux ratio	0.01	0.02	0.03	0.06	0.08	0.12	0.17	0.34	$mol \, mol^{-1}$
Reboiler duty	5443	5091	4706	4385	4019	3598	3081	2548	kW
Condenser duty	− 5212	− 4661	− 4141	− 3611	− 3066	− 2521	− 1969	− 1470	kW
Total Duty									
Heating	7191	8002	8798	9574	10,112	10,752	11,290	11,712	kW
Cooling	− 7093	− 7883	− 8680	− 9464	− 10,013	− 10,666	− 11,219	− 11,659	kW
Capital Cost (CAPEX)									
Column	1.08	1.53	1.94	1.93	2.13	2.08	2.19	2.10	M $
Reboiler	1.21	1.32	1.41	1.50	1.56	1.63	1.69	1.73	M $
Condenser	1.09	1.18	1.29	1.41	1.51	1.63	1.74	1.84	M $
Operating Cost (OPEX)									
Heating	3.66	3.96	4.26	4.55	4.74	4.97	5.14	5.26	M $ y^{-1}
Cooling	0.08	0.08	0.09	0.10	0.11	0.11	0.12	0.12	M $ y^{-1}
Overall									
CAPEX	3.39	4.03	4.65	4.84	5.20	5.34	5.62	5.66	M $
Ann. CAPEX	0.42	0.50	0.58	0.61	0.65	0.67	0.70	0.71	M $ y^{-1}
OPEX	3.73	4.05	4.35	4.65	4.85	5.08	5.26	5.38	M $ y^{-1}
TAC	4.16	4.55	4.93	5.26	5.50	5.75	5.96	6.09	M $ y^{-1}

(a) Extractive process

(b) Hybrid process

Fig. 6 – The optimal structures for the extractive and hybrid processes for a feed composition of 0.30 ethanol. Note that the condenser is the first stage and the reboiler is the last stage.

flow rate, which contains mainly ethanol (since the azeotropic point is near $0.90\,mol\,mol^{-1}$ ethanol), increases accordingly. The reflux ratio shows the opposite trend, i.e., the optimal reflux ratio decreases as the feed composition increases. The reboiler duty, on the other hand, increases as there is an overall increase in the total liquid flow within the column (i.e., the sum of the fresh feed, recycled entrainer (recovery flow rate), and reflux), due to the increase in the internal entrainer flow rate which is required as there is more ethanol, and therefore azeotrope, in the system and more entrainer is needed to break the azeotrope. As for the condenser duty, the increase in ethanol composition leads to

a larger distillate flow rate, thus more energy is required to condense the distillate.

Considering the entrainer recovery column, column C2, the total number of stages is low and relatively constant, and the feed is almost always at the mid-point of the column. The total number of stages stays relatively constant as the feed flow rate into the recovery column, the bottom stream from column C1, remains almost the same (ranging from about $467\,kmol\,h^{-1}$ to $482\,kmol\,h^{-1}$, not shown in the table). In general, the reflux ratio required in the recovery column is very low, but there is an overall increase in the reflux ratio with increasing feed composition. Both the reboiler duty and the

(a) Extractive process

(b) Hybrid process (base)

(c) Hybrid process (half cost)

(d) Hybrid process (90 °*C*)

Fig. 7 – Stacked bar showing the annualised capital cost (CAPEX) and operating cost (OPEX) for each of the processes studied together with the elements that make up the CAPEX and OPEX.

condenser duty decrease as the feed composition increases. Overall, the total heating and cooling duties required by the extractive process increase as the feed composition increases, as the impact of the reboiler and condenser duties of the extractive column is larger than those of the recovery column.

In terms of economic performance, a gradual increase in CAPEX and OPEX, thus a gradual increase in TAC, can be observed as the feed ethanol composition increases, by about 46% as the feed composition increases from 0.1 to 0.8. It should be noted that, although the design for a feed composition of 0.1 has a similar total number of stages of the first column compared with that of a feed composition of 0.8, the CAPEX of the column for 0.8 is almost doubled. This is due to much higher liquid and vapour flows in the first column for a feed composition of 0.8 due to the larger amount of entrainer, resulting in a column with a larger column diameter and, therefore, a much higher CAPEX (see the distillation sizing and costing equations in the appendix of Duanmu et al. (2022b). From the stacked bar results (shown in Fig. 7a) and the corresponding donut chart (shown in Fig. S1), the relative contribution of distillation columns, condensers, and reboilers to CAPEX is almost the same, with the distillation column having a slightly higher weight than the other two combined. For the OPEX, which is made up of heating and cooling utility costs, it can be seen that the heating utility cost makes up the majority of the OPEX, and therefore the major contribution of the TAC (about 86%), as the cost of the

heating utility (low-pressure steam in this case) is much higher than the cooling utility. Moreover, due to the high heating utility cost, the OPEX contributes about 88% of the TAC. From the economic analysis it can be deduced that, in order to improve the economic performance of the extractive process, the focus should be on implementing heat integration for more efficient energy usage, however, this is not considered in this work.

3.3. Optimal design of a hybrid process

Next, consider the hybrid process for the same separation. The optimal results are given in Table 4 for different feed compositions of ethanol, and an example flowsheet for the optimal hybrid process at a molar feed composition 0.30 ethanol is shown in Fig. 6b. It can be seen that the total number of stages in the distillation column reaches a peak at a composition of 0.4, which makes sense for the same reasons as discussed for extractive distillation above. The feed stage location of the fresh feed stream changes gradually from near the bottom to near the top, which indicates that the optimal design has the feed entering at a stage with a composition close to that of the feed composition to minimise the mixing effect (i.e., maximise energy efficiency).

The reflux ratio decreases with increasing feed composition, which was also observed for the extractive distillation process. Equally, the distillate flow rate also increases due to more light component entering the system. It is interesting

Table 4 – Optimal results for the base case hybrid distillation-pervaporation process at different ethanol feed compositions. See the key membrane parameters in Table 1.

Item	Feed Ethanol Molar Composition								Units
	0.10	0.20	0.30	0.40	0.50	0.60	0.70	0.80	
Column C1									
Total stages	22	23	26	27	24	18	16	17	–
Feed stage	17	18	22	22	18	10	6	3	–
Recycle stage	21	20	25	23	21	17	13	15	–
Distillate	57.77	121.27	185.34	249.28	311.88	391.49	462.83	489.23	$kmol\,h^{-1}$
Reflux ratio	1.15	1.12	1.01	0.97	1.03	0.62	0.11	0.11	$mol\,mol^{-1}$
Reboiler duty	1437	2888	4132	5401	6891	6935	5571	5882	kW
Condenser duty	− 1343	− 2777	− 4028	− 5313	− 6820	− 6887	− 5544	− 5869	kW
Membrane Network [*]									
No. membrane stages	7	6	8	8	$10^{\dagger}$	$10^{\dagger}$	$10^{\dagger}$	$10^{\dagger}$	–
No. modules in stage 1	9	33	33	40	30	67	95	61	–
No. modules in stage 2	12	22	23	24	44	44	81	81	–
No. modules in stage 3	14	40	41	52	73	81	94	90	–
No. modules in stage 4	12	49	51	55	43	50	84	116	–
No. modules in stage 5	23	62	37	73	55	101	111	106	–
No. modules in stage 6	33	104	60	124	58	73	112	126	–
No. modules in stage 7	39	–	75	136	51	98	99	148	–
No. modules in stage 8	–	–	124	96	103	148	133	111	–
No. modules in stage 9	–	–	–	–	142	106	144	130	–
No. modules in stage 10	–	–	–	–	122	149	137	150	–
Total no. modules	142	310	444	600	721	917	1090	1119	–
Total membrane area	852	1860	2664	3600	4326	5502	6540	6714	m^2
Membrane heating duty	149	298	466	648	794	1184	1460	1090	kW
Distillate cooling duty	− 18	− 39	− 59	− 79	− 99	− 124	− 146	− 157	kW
Permeate cooling duty	− 156	− 316	− 488	− 664	− 818	− 1185	− 1443	− 1135	kW
Permeate heating duty	27	54	83	113	140	203	248	193	kW
Total Duty									
Heating	1613	3240	4681	6162	7825	8322	7279	7165	kW
Cooling	− 1517	− 3132	− 4575	− 6056	− 7737	− 8196	− 7134	− 7160	kW
Capital Cost (CAPEX)									
Column	0.42	0.53	0.78	0.89	0.95	0.69	0.50	0.56	M $
Membrane	4.67	10.20	14.60	19.73	23.71	30.16	35.85	36.80	M $
Reboiler	0.34	0.53	0.68	0.82	0.99	1.00	0.84	0.88	M $
Condenser	0.26	0.43	0.60	0.79	1.02	1.03	0.82	0.87	M $
Others	1.28	1.17	1.46	1.49	1.78	1.86	1.91	1.85	M $
Operating Cost (OPEX)									
Heating	0.69	1.38	1.99	2.62	3.32	3.54	3.09	3.04	$M\,\$\,y^{-1}$
Cooling	0.05	0.11	0.16	0.22	0.27	0.36	0.41	0.34	$M\,\$\,y^{-1}$
Electricity	0.00	0.00	0.00	0.00	0.00	0.00	0.00	0.00	$M\,\$\,y^{-1}$
Mem. Replacement	0.13	0.29	0.41	0.55	0.66	0.84	1.00	1.03	$M\,\$\,y^{-1}$
Overall									
CAPEX	6.96	12.85	18.12	23.73	28.45	34.73	39.93	40.96	M $
Ann. CAPEX	0.87	1.61	2.26	2.97	3.56	4.34	4.99	5.12	$M\,\$\,y^{-1}$
OPEX	0.87	1.77	2.56	3.39	4.26	4.74	4.51	4.41	$M\,\$\,y^{-1}$
TAC	1.74	3.38	4.82	6.35	7.82	9.08	9.50	9.53	$M\,\$\,y^{-1}$

[*] Existence of the membrane feed heater is also optimised. The heaters exist only between the second to membrane stage N_{ms}^{opt} for all designs. [†] Upper bound of the variable

to note that all optimal designs tend to achieve only about 0.8 molar composition of ethanol in the distillate (not shown in the table). Even when the feed composition is 0.8, the distillate composition is only about 0.82. This is expected when considering the VLE diagram for the mixture, as after a composition of about 0.8, the bubble point and dew point of the mixture become very close, leading to a difficult separation. Thus, continuing the separation using the distillation column would be costly as a large amount of heating and cooling would be required.

For each design, the energy consumption of the reboiler and condenser contributes the most to the total heating and cooling (up to 89%), and a peak in the duty is noticed at a feed composition of 0.6. This peak is probably the result of a trade-off between an easier separation (close to the target, i.e. azeotropic, composition) and a higher amount of light component needed to be boiled up.

Regarding the membrane network, it is clear that the number of membrane stages and total membrane modules increase with the feed composition as more material needs to be handled by the network as the distillate flow rate from the column increases. (Note that the maximum number of stages considered was 10, i.e. the upper bound on N_{ms} = 10.) It can be seen that the total heating duty for a feed composition of 0.8 is smaller than the duty for 0.7. This is because the distillate for both cases is close, but the purity of the distillate

for 0.7 (0.76 molar composition) is smaller than for 0.8 (0.82 molar composition) leading to a more difficult separation and therefore higher energy duty required.

The cost comparison can be seen in the stacked bar results (shown in Fig. 7b) and the corresponding donut chart (shown in Fig. S2). In terms of the CAPEX, the membrane system (i.e., the cost of the membrane modules) always contributes the most with up to 90% of the CAPEX. As an example, the cost of the membrane modules is 70 times higher than the cost of the distillation column (shell and trays) for a feed composition of 0.7. The membrane cost increases with the feed composition due to more membrane modules being required to handle the larger membrane feed amounts. For feed compositions higher than 0.5, the cost of the distillation column is even lower than that of the reboiler and condenser due to the large energy consumption requiring a large reboiler and condenser. It should be noted that units classified as "others", which include the pump, heaters on each membrane stage, permeate cooler, permeate heater, and distillate cooler, play the second most important role in the CAPEX. However, it is still significantly less than the cost of the membrane system, especially when the feed composition is high. Focusing on the OPEX, it is not surprising that the heating contributes the most due to the higher cost of the low-pressure steam used in the heaters and the reboiler compared to the cooling water used in the condenser. Even though refrigerant (– 20°C) is used in the permeate cooler, the duty is still less than the heating requirements. The cost of membrane replacement increases with the feed composition and is the second highest cost in the OPEX.

Considering the total annualised cost (TAC), general speaking, the OPEX and annualised CAPEX contribute almost equally for the hybrid process (OPEX ranges from about 46–54%) without a clear trend as the feed composition increases. However, the contribution of the annualised CAPEX of the membrane modules to TAC increases from approximate 34–48%, indicating that the membrane system is one of the key factors affecting the CAPEX and TAC. In contrast to the extractive distillation process, the TAC varies significantly, from $ 1.74\,M\,y^{-1}$ to $ 9.53\,M\,y^{-1}$, showing that the hybrid process is very sensitive to the feed condition and this is a key finding of this work.

3.3.1. Impact of key membrane parameters

The previous investigation has shown that the membrane characteristics, particularly the membrane cost, has a significant impact on the optimal design. In the following we will therefore briefly consider the impact of both membrane cost and maximum allowable membrane temperature on the hybrid process performance. The impact of membrane costs (denoted *hybrid process (half cost)*) is investigated by considering a membrane with half the capital and operating cost compared to the base case, while the impact of maximum membrane temperature (denoted *hybrid process (90 °C)*) is investigated by increasing this from 70 °C to 90 °C.

The findings for both hybrid process variations (half cost or 90°C) in terms of their designs are similar to those found in Section 3.3 (see Table 5 and Table 6 as well as Fig. S3 and Fig. S4). Compared to the base case hybrid process, the designs for half the membrane cost (such as the total number of stages, reflux ratio, membrane system, and energy consumption) have only minor differences. This finding is not surprising because, although the membrane cost is halved,

the membrane cost is still significantly higher than the CAPEX of the other units (see Fig. S3), therefore the membrane is still the most dominant factor affecting the hybrid design, as it was for the base case.

For the hybrid process with a higher allowable temperature (90°C), although the membrane performance is improved, the membrane system still contributes the most to the CAPEX (see Fig. S4). The stacked bar results (see Fig. 7) and the donuts charts for both processes (see Fig. S3 and S4) indicate that total CAPEX (especially for the membrane system) drops significantly. For example, compared with the based case hybrid process, the contribution of the CAPEX to the TAC of the hybrid process (half membrane cost) and hybrid process (maximum temperature 90°C) drops from about 50–40% and 30%, respectively. This indicates that improving the membrane performance may be a efficient way to reduce the overall cost, however, a more comprehensive comparison would be needed, considering various membrane properties, to fully investigate this impact.

3.4. Process comparison

A comparison of the total number of stages in the extractive process (sum of the number of stages in both columns) and the hybrid distillation-pervaporation process shows that the total number of stages in the distillation column of the hybrid process is much smaller (16–28 total number of stages in the hybrid process compared to 41–52 stages in the extractive process), as the hybrid process only requires one column as there is no entrainer to recover. Considering the total heating and cooling duties (summation of individual duties utilised for each relevant unit), shown in Fig. 8a and Fig. 8b, respectively, the energy consumption in the extractive process is always higher than that of the hybrid process, indicating that the hybrid process is always superior in terms of energy consumption. This finding is consistent with the findings in the literature (Lipnizki et al., 1999; Van Hoof et al., 2004; Tgarguifa et al., 2018). In addition, the hybrid process design for the base case, and those of the hybrid variations, have similar energy consumptions except for the case of a feed composition of 0.6, where the difference is more significant than for the other feed compositions. This finding is most likely due to the trade-off between the CAPEX and OPEX as explained in Section 3.3 for the turning point in energy consumption. Moreover, Fig. 8a and Fig. 8b also show that the saving in energy consumption is more significant for the hybrid process at extreme feed compositions as discussed above for the individual processes.

In terms of the economic performance, Fig. 8c shows the change in CAPEX with the increase in feed composition. It is clear that the CAPEX of the extractive process remains almost constant and is almost always lower than for the hybrid process. Even for the hybrid process with halved membrane cost or higher maximum temperature, the CAPEX for the extractive process is still significantly lower. As discussed in Section 3.3.1, improving the membrane performance is clearly the main way to reduce the cost of the hybrid process. Considering the OPEX (shown in Fig. 8d), it is not surprising that the change in OPEX follows a similar trend to that of the energy consumption. It should be noted that the gap between the OPEX of the hybrid and extractive processes becomes narrower as the feed composition increases, likely due to the different heating and/or cooling utilities used. For example, cooling water is used in the condensers in the extractive

Table 5 – Optimal results for the hybrid distillation-pervaporation process with half the membrane costs at different ethanol feed compositions. See the key membrane parameters in Table 1.

Item	Feed Ethanol Molar Composition								Units
	0.10	0.20	0.30	0.40	0.50	0.60	0.70	0.80	
Column C1									
Total stages	20	19	28	26	24	18	17	17	–
Feed stage	16	16	23	22	18	10	5	3	–
Recycle stage	20	19	27	25	23	18	16	12	–
Distillate	57.43	122.99	186.71	249.34	314.33	395.84	459.66	489.40	$kmol\,h^{-1}$
Reflux ratio	1.24	1.03	0.92	0.99	0.95	0.51	0.12	0.12	$mol\,mol^{-1}$
Reboiler duty	1482	2814	3978	5437	6702	6533	5594	5892	kW
Condenser duty	– 1388	– 2704	– 3876	– 5348	– 6631	– 6490	– 5572	– 5880	kW
Membrane Network *									
No. membrane stages	5	7	7	9	$10^{\dagger}$	$10^{\dagger}$	$10^{\dagger}$	$10^{\dagger}$	–
No. modules in stage 1	19	17	50	50	49	49	64	66	–
No. modules in stage 2	21	21	36	21	33	45	61	87	–
No. modules in stage 3	21	36	46	48	87	43	91	86	–
No. modules in stage 4	47	32	51	50	58	64	104	114	–
No. modules in stage 5	47	35	48	60	61	89	79	122	–
No. modules in stage 6	–	59	106	69	32	130	119	130	–
No. modules in stage 7	–	105	125	114	75	137	146	139	–
No. modules in stage 8	–	–	–	105	115	149	128	143	–
No. modules in stage 9	–	–	–	86	102	116	136	99	–
No. modules in stage 10	–	–	–	–	123	107	146	136	–
Total no. modules	155	305	462	603	735	929	1074	1122	–
Total membrane area	930	1830	2772	3618	4410	5574	6444	6732	m^2
Membrane heating duty	144	320	491	626	827	1264	1425	1096	kW
Distillate cooling duty	– 18	– 39	– 59	– 79	– 100	– 125	– 145	– 157	kW
Permeate cooling duty	– 151	– 338	– 508	– 660	– 846	– 1251	– 1418	– 1138	kW
Permeate heating duty	26	58	87	113	145	214	243	194	kW
Total Duty									
Heating	1652	3192	4556	6176	7674	8011	7262	7182	kW
Cooling	– 1557	– 3081	– 4444	– 6087	– 7577	– 7866	– 7135	– 7175	kW
Capital Cost (CAPEX)									
Column	0.37	0.41	0.85	0.85	0.93	0.59	0.54	0.56	$M\,\$$
Membrane	2.55	5.02	7.60	9.92	12.09	15.28	17.66	18.45	$M\,\$$
Reboiler	0.35	0.52	0.66	0.83	0.97	0.95	0.85	0.88	$M\,\$$
Condenser	0.26	0.42	0.58	0.79	0.99	0.97	0.83	0.87	$M\,\$$
Others	1.02	1.30	1.33	1.49	1.79	1.87	1.91	1.85	$M\,\$$
Operating Cost (OPEX)									
Heating	0.70	1.36	1.94	2.62	3.26	3.40	3.09	3.05	$M\,\$\,y^{-1}$
Cooling	0.05	0.11	0.16	0.22	0.28	0.37	0.40	0.34	$M\,\$\,y^{-1}$
Electricity	0.00	0.00	0.00	0.00	0.00	0.00	0.00	0.00	$M\,\$\,y^{-1}$
Mem. Replacement	0.07	0.14	0.21	0.28	0.34	0.43	0.49	0.52	$M\,\$\,y^{-1}$
Overall									
CAPEX	4.55	7.67	11.02	13.88	16.77	19.66	21.78	22.61	$M\,\$$
Ann. CAPEX	0.57	0.96	1.38	1.73	2.10	2.46	2.72	2.83	$M\,\$\,y^{-1}$
OPEX	0.82	1.61	2.31	3.12	3.88	4.21	3.98	3.91	$M\,\$\,y^{-1}$
TAC	1.39	2.57	3.69	4.85	5.97	6.66	6.71	6.74	$M\,\$\,y^{-1}$

* Existence of membrane feed heater is also optimised. The heaters exist only between the second to membrane stage N_{ms}^{opt} for all designs, except for the design for 0.40 feed ethanol molar composition where the heater on stage nine is also absent. $\dagger$ Upper bound of the variable

process, and it is the only cooling utility. However, in the hybrid process, a refrigerant is used in the membrane network to condense the permeate, and this cost is much higher than for the cooling water. (It should be noted that the selection of the type of utility source is automated during the optimisation.) The stacked bar results (shown in Fig. 7) and donut charts (shown in Fig. S1 to S4), demonstrate that for the extractive process, the OPEX contributes the most to the TAC (about 90%), however, for the hybrid process this drops to about 50%, not only due to the reduced OPEX cost in the hybrid process but also due to the higher CAPEX caused by the expensive membrane network. With the hybrid process with the modified characteristics, the contribution of OPEX to

TAC is increased to about 60% and 70% for half membrane cost and increased maximum temperature (90°C), respectively. For all processes, the heating cost dominates the OPEX.

Overall, looking at the trend of the TAC (shown in Fig. 8e and Fig. 8f), there is a clear flipping point (at about 0.3 $mol\,mol^{-1}$)) when the extractive process becomes cheaper than the based case hybrid process. At low ethanol feed compositions, the TAC of the based case hybrid process is much cheaper, up to about 57% lower, while on the other hand, the based case hybrid process can be up to about 59% more expensive at high ethanol feed compositions. By halving the membrane cost, the flipping point shifts to about 0.45 mol

Table 6 – Optimal results for the hybrid distillation-pervaporation process at higher maximum allowable membrane temperature (90°C) at different ethanol feed compositions. See the key membrane parameters in Table 1.
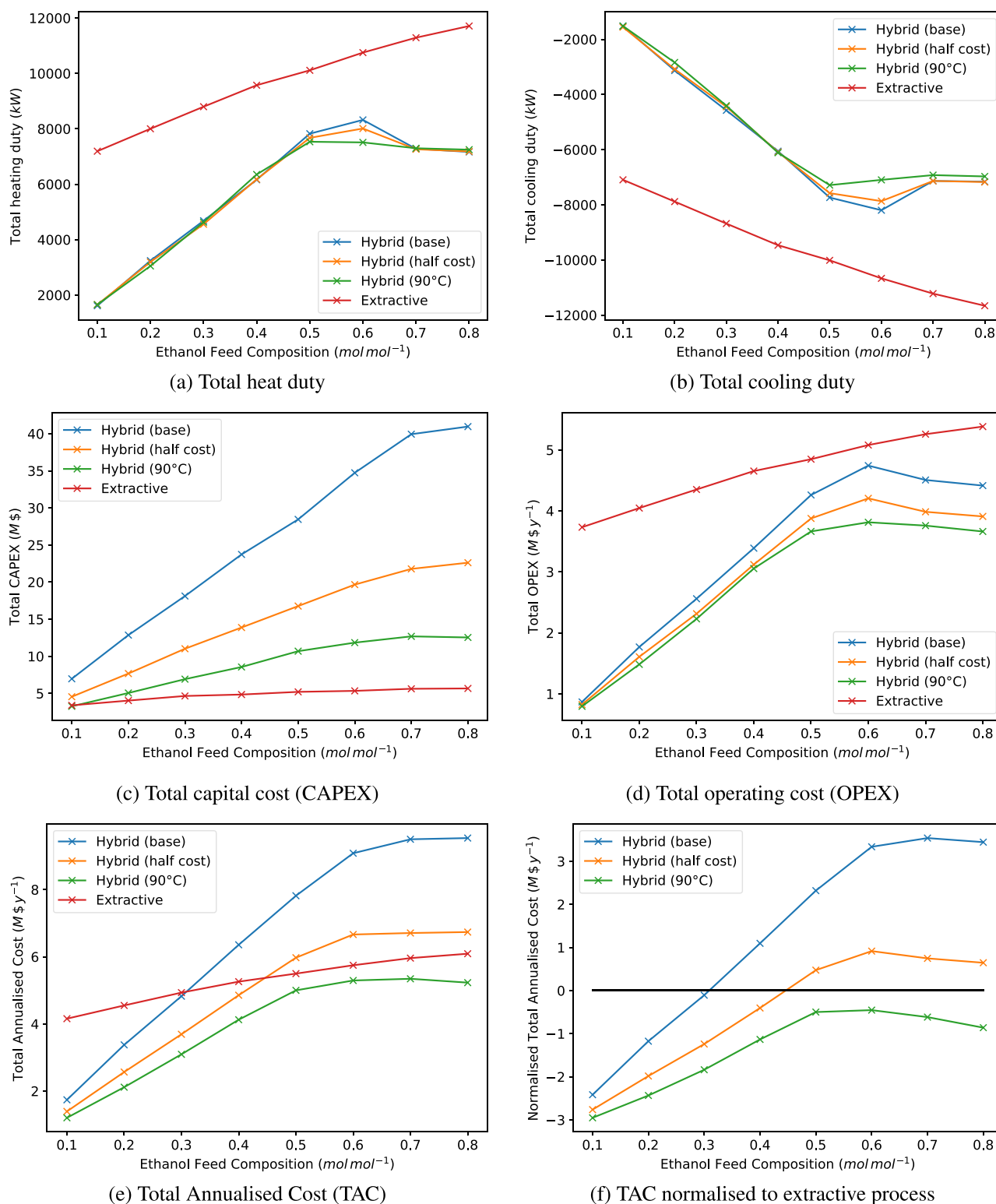
| | Feed Ethanol Molar Composition | | | | | | | | |
Item	0.10	0.20	0.30	0.40	0.50	0.60	0.70	0.80	Units
Column C1									
Total stages	18	20	28	23	25	18	16	17	–
Feed stage	14	17	24	19	21	9	9	6	–
Recycle stage	18	20	28	23	24	17	16	16	–
Distillate	58.11	124.80	185.84	247.31	313.87	406.57	459.05	488.02	$kmol\,h^{-1}$
Reflux ratio	1.16	0.83	0.95	1.05	0.90	0.29	0.10	0.11	$mol\,mol^{-1}$
Reboiler duty	1448	2572	4011	5552	6498	5727	5506	5847	kW
Condenser duty	−1355	−2467	−3909	−5467	−6433	−5693	−5493	−5840	kW
Membrane Network*									
No. membrane stages	4	6	6	5	5	8	7	7	–
No. modules in stage 1	11	9	9	19	22	21	26	14	–
No. modules in stage 2	14	10	9	21	16	22	32	38	–
No. modules in stage 3	8	10	15	23	49	13	21	24	–
No. modules in stage 4	11	16	24	40	36	28	16	20	–
No. modules in stage 5	–	18	17	51	80	45	39	24	–
No. modules in stage 6	–	15	36	–	–	24	63	47	–
No. modules in stage 7	–	–	–	–	–	35	77	100	–
No. modules in stage 8	–	–	–	–	–	53	–	–	–
No. modules in stage 9	–	–	–	–	–	–	–	–	–
No. modules in stage 10	–	–	–	–	–	–	–	–	–
Total no. modules	44	78	110	154	203	241	274	267	–
Total membrane area	264	468	660	924	1218	1446	1644	1602	m^2
Membrane heating duty	177	413	533	690	890	1544	1549	1209	kW
Permeate cooling duty	−162	−372	−497	−644	−853	−1402	−1430	−1131	kW
Permeate heating duty	28	63	84	109	145	239	243	192	kW
Total Duty									
Heating	1652	3049	4627	6351	7533	7510	7298	7247	kW
Cooling	−1517	−2839	−4406	−6111	−7286	−7095	−6923	−6970	kW
Capital Cost (CAPEX)									
Column	0.32	0.42	0.85	0.74	0.97	0.57	0.50	0.56	$M\,\$$
Membrane	1.45	2.57	3.62	5.07	6.68	7.93	9.01	8.78	$M\,\$$
Reboiler	0.35	0.49	0.66	0.84	0.95	0.86	0.84	0.87	$M\,\$$
Condenser	0.26	0.39	0.58	0.81	0.96	0.84	0.81	0.87	$M\,\$$
Others	0.89	1.18	1.20	1.10	1.14	1.64	1.52	1.46	$M\,\$$
Operating Cost (OPEX)									
Heating	0.70	1.30	1.97	2.70	3.20	3.19	3.10	3.08	$M\,\$\,y^{-1}$
Cooling	0.05	0.12	0.16	0.21	0.27	0.40	0.40	0.34	$M\,\$\,y^{-1}$
Electricity	0.00	0.00	0.00	0.00	0.00	0.00	0.00	0.00	$M\,\$\,y^{-1}$
Mem. Replacement	0.04	0.07	0.10	0.14	0.19	0.22	0.25	0.25	$M\,\$\,y^{-1}$
Overall									
CAPEX	3.26	5.05	6.92	8.56	10.69	11.84	12.68	12.54	$M\,\$$
Ann. CAPEX	0.41	0.63	0.86	1.07	1.34	1.48	1.59	1.57	$M\,\$\,y^{-1}$
OPEX	0.80	1.48	2.23	3.05	3.66	3.81	3.76	3.66	$M\,\$\,y^{-1}$
TAC	1.20	2.11	3.09	4.12	5.00	5.29	5.34	5.23	$M\,\$\,y^{-1}$

*Existence of membrane feed heater is also optimised. The heaters exist only between the first to membrane stage N_{ms}^{opt} for all designs.

mol^{-1}. For a higher temperature tolerant membrane, the hybrid process is cheaper than the extractive process for all compositions. This result indicates the great economic potential of the hybrid process if the performance and cost of the membrane unit is beneficial. The result also shows the importance of properly investigating the impact of feed composition before drawing conclusions as to which process is the best. Previously, Kanchanalai et al. (2012) compared two hybrid distillation-membrane processes, which uses pervaporation membrane or vapour permeation membrane, for the same systems with different feed concentrations (compositions). Their results showed that the hybrid distillation-vapour permeation processes would be more beneficial than the hybrid distillation-pervaporation process at higher feed concentrations. Coupled with the finding in this work, after the flipping point, if a hybrid distillation-vapour permeation process is used instead of

the hybrid distillation-pervaporation process, the hybrid distillation-membrane process may still be economically more attractive than the extractive process. However, further exploration and optimisation are required to conduct a valid conclusion.

It should be noted that both the hybrid process and extractive distillation may be improved. For example, in this work, the permeate side pressure is 400 Pa, which is taken from the experimental setup (Tsuyumoto et al., 1995), resulting in the usage of the expensive −20°C refrigerant in the permeate cooler. This may be improved by using a higher permeate pressure, thus allowing for the use of cheap cooling water as the cooling utility. However, the trade-off between the decrease in performance due to increased permeate side pressure and the decrease in cooling utility cost should be carefully evaluated. For extractive distillation, an extra column at the beginning to pre-concentrate the feed may help with the separation and economic performance,

(a) Total heat duty

(b) Total cooling duty

(c) Total capital cost (CAPEX)

(d) Total operating cost (OPEX)

(e) Total Annualised Cost (TAC)

(f) TAC normalised to extractive process

Fig. 8 – Comparison of the economic performances (TAC, CAPEX, and OPEX) and duties (heating and cooling) required for the extractive and hybrid processes (base case, half membrane cost and increased membrane temperature tolerance).

however, the additional column will introduce an additional capital cost. Moreover, the decision of whether or not to add the extra column will make the optimisation of the extractive distillation into a superstructure problem.

4.   Conclusion

In this work, we have presented three strategies for how to construct a membrane network superstructure model,

consisting of multiple membrane stages with variable number of membrane modules per stage, and we have provided a recommendation for the most efficient strategy to minimise numerical difficulties related to initialisation and convergence. The superstructure representation was found to provide optimal results with a fraction of the solution time compared to repeated optimisation for each number of stages.

We have also considered the optimal design of both an extractive distillation process and a hybrid distillation-pervaporation process for the separation of a minimum-boiling azeotropic system, considered for a range of feed compositions and also briefly investigated the impact of membrane cost and maximum membrane temperature. The results showed that the hybrid process can always save energy, however, a flipping point exists in terms of total annualised costs in terms of feed composition, below which the hybrid process is the cheapest but above which the extractive process is preferred.

Declaration of Competing Interest

The authors declare that they have no known competing financial interests or personal relationships that could have appeared to influence the work reported in this paper.

Acknowledgements

Appendix A. Supporting information

Supplementary data associated with this article can be found in the online version at doi:10.1016/j.cherd.2023.04.014.

Appendix B. Membrane Model Equations

This section contains the assumptions and modelling equations for the pervaporation membrane model used in this work. As the purpose of this study is to investigate the optimal design of a hybrid dividing wall column, a steady-state model for the membrane will suffice. Some assumptions made for the pervaporation membrane are:

1. The flow pattern in the membrane is co-current flow (Li et al., 2019).
2. Feed is fed into the membrane at the tube side, while permeate is collected from the shell side.
3. Ideal gas state on the permeate side.
4. No pressure drop at the permeate side.
5. Temperatures of the retentate and permeate in a membrane fragment are the same, i.e., the temperature is constant in a membrane fragment (Luyben, 2009; Liu et al., 2022; Zhao et al., 2022).

Instead of modelling the membrane as a distributed model, a lumped model where a membrane module is divided into smaller membrane fragments is used to simulate the mass and energy distribution across the membrane. This lumped model approach is widely reported in the open literature and is reported to be sufficient for the modelling of a membrane model (Luyben, 2009; Li et al., 2019; Meng et al., 2020; Wu et al., 2020). Through validation with experimental (Tsuyumoto et al., 1997) and simulation (Marriott, 2001) results, it was found that dividing a membrane module into nine membrane fragments, i.e., $N_{frag.} = 9$, is sufficient to describe the membrane (see model validation results in Table A1).

The membrane used in this work are taken from Marriott and Sorensen (2003a) and Tsuyumoto et al. (1997). The details

of the membrane are shown in Table A2. It should be noted that in Tsuyumoto et al. (1997), the membrane area of $6\,m^2$ is the effective membrane area at about 75% efficiency, but Marriott and Sorensen (2003a) took the $6\,m^2$ as the 100% effective membrane area (which is also used in this work). Therefore, instead of directly taking the fibre radius from Tsuyumoto et al. (1997), Marriott and Sorensen (2003a) (and this work) recalculated the fibre radius from $6\,m^2$ and 3800 fibres:

$$
\begin{aligned}
A_{mem} &= (2\,\pi\,r_{fibre}\,L_{mem})N_{fibre} \\
r_{fibre} &= \frac{(A_{mem}/N_{fibre})}{2\,\pi\,L_{mem}} \\
&= \frac{6/3800}{2\,\pi \times 1} \\
&= 2.51 \times 10^{-4}\,m
\end{aligned}
\tag{A1}
$$

In the following equations, the subscripts i denotes the component i (or specifically w for water and e for ethanol), *feed* denotes the feed side, *ret* denotes the retentate side, *perm* denotes the permeate side, and *mem* denotes the membrane layer, and the term N_{comp} denotes the number of components.

A.1. Membrane fluxes

One of the most important equations in a membrane model is the flux equation. Each membrane has its own flux equation, and this work reports only the flux equation used in the case study for the separation of an ethanol/water mixture, which is obtained from Tsuyumoto et al. (1997) for a polyacrylonitrile ultrafiltration hollow-fibre membrane PAN-B5. The necessary information for the membrane can be found in Table A2. A solution-diffusion approach is used to formulate the equation for the flux of water through the membrane, J_W ($g\,m^{-2}\,h^{-1}$), which is given by:

$$
\begin{aligned}
J_w &= \frac{D_{w0}\,K_{cw}}{\delta}\left(\gamma_{feed,w}\,x_{feed,w} - \frac{P_{perm}\,x_{perm,w}}{P_w^{sat}}\right)^2 \\
&\quad + \left(\frac{D_{w0}\,K_{cw}^2\,k_{dw}}{2\delta}\right)\left[(\gamma_{feed,w}\,x_{feed,w})^2 - \left(\frac{P_{perm}\,x_{perm,w}}{P_w^{sat}}\right)^2\right]
\end{aligned}
\tag{A2}
$$

where the subscripts *feed* denotes the feed side, *perm* denotes the permeate side, and w denotes water, and the terms D_{w0} is the diffusion coefficient of water at infinite dilution, K_{cw} is the sorption coefficient, k_{dw} is a numerical constant, δ is the membrane thickness, γ is the activity coefficient, x is the molar composition, P is the pressure, and P^{sat} is the saturated vapour pressure. γ and P^{sat} are obtained from Multiflash (KBC Advanced Technologies, 2015).

Table A1 – Comparison of the results obtained from the lumped model in this work with experimental (Tsuyumoto et al., 1997) and the 1D and 2D distributed model (Marriott (2001) for two case studies with different feed conditions.

Feed flow rate ($kg\,h^{-1}$)	44.8	248.5
Feed ethanol composition ($kg\,kg^{-1}$)	0.940	0.968
Tsuyumoto et al. (1997)	0.972	0.974
Marriott (2001) 1D model	0.975	0.974
Marriott (2001) 2D model	0.973	0.974
This work lumped model	0.970	0.973

Table A2 – Details of the pervaporation membrane used (Marriott and Sorensen, 2003a).

Items	Values	Units
Membrane thickness, δ	1.5	μm
Membrane length, L_{mem}	1	m
Membrane area, A_{mem} *	6	m^2
Shell radius, r_{shell} (inner)	48.7	mm
Fibre radius, r_{fibre} (inner)†	0.251	mm
Number of fibres, N_{fibre}	3800	–

* 100% efficient membrane area † Recalculated using Equation (A1).

The equation for the flux of ethanol through the membrane, J_e ($g\,m^{-2}\,h^{-1}$), can, however, be described with a simple equation:

$$J_e = L_p\,\omega_{feed,e}\left(P_{feed} - P_{perm}\right) \tag{A3}$$

where the subscripts *feed* denotes the feed side, *perm* denotes the permeate side, and *e* denotes ethanol, and the terms L_p is the permeability constant which is membrane-dependent, ω is the mass fraction, and P is the pressure. Tsuyumoto et al. (1997) claimed that an average value where $L_p = 5 \times 10^{-3}\,g\,m^{-2}\,h^{-1}\,torr^{-1}$ could be used for the membrane used in this work.

The terms $(D_{w0}\,K_{cw})$ and $(D_{w0}\,K_{cw}^2\,k_{dw}/2)$ in the water flux equation (Equation (A2)) are given by the equations below (Tsuyumoto et al., 1997):

$$D_{w0}\,K_{cw} = 5.24 \times 10^{11}\exp\left(\frac{-1150}{T_{feed}}\right) \tag{A4}$$

$$\frac{D_{w0}\,K_{cw}^2\,k_{dw}}{2} = 223\exp\left(\frac{-3390}{T_{feed}}\right) \tag{A5}$$

where T_{feed} is the temperature at the feed side.

A.2. Molar balance equations

The component molar balances at the retentate and permeate sides are given by the equations below:

$$\frac{dx_{ret,i}}{dt} = \frac{F_{feed}\,x_{feed,i} - F_{ret}\,x_{ret,i} - A_{fibre}\,J_i}{M_{ret}} \quad \forall\,i = 1,\,...,N_{comp} \tag{A6}$$

$$\frac{dx_{perm,i}}{dt} = \frac{-F_{perm}\,x_{perm,i} + A_{fibre}\,J_i}{M_{perm}} \quad \forall\,i = 1,\,...,N_{comp} \tag{A7}$$

where x is the molar composition, F is the molar flow rate, A_{fibre} is the surface area of the fibre, J is the flux, and M is the molar holdup. The surface area of the fibre is calculated by

$$A_{fibre} = \frac{A_{mem}}{N_{fibre}} \tag{A8}$$

where A_{mem} is the membrane area.

Then, under a steady-state condition:

$$F_{feed}\,x_{feed,i} = F_{ret}\,x_{ret,i} + A_{fibre}\,J_i \tag{A9}$$

$$F_{perm}\,x_{perm,i} = A_{fibre}\,J_i \tag{A10}$$

A.3. Pressure drop equations

In this work, the permeate side pressure is maintained at a $400\,Pa$ (Tsuyumoto et al., 1997), and it is assumed that the pressure drop across the membrane at the permeate side is negligible (Assumption 4). For the retentate side, which is at

the fibre side (Assumption 2), one of the most commonly used equations to calculate the pressure drop is the Hagen-Poiseuille equation for laminar flow (Pan, 1986; Lipski and Coˇté, 1990; Marriott, 2001; Kookos, 2002; Katoh et al., 2011; Li et al., 2019):

$$\Delta P_{ret} = \frac{8\,\mu_{fibre}\,L_{mem}\,\dot{V}_{ret}}{\pi r_{fibre}^2} \tag{A11}$$

where the subscript *fibre* denotes the fibre side, the terms ΔP is the pressure change/drop, μ is the dynamic viscosity of the liquid, L_{mem} is the length of the membrane module, $\dot{V}$ is the volumetric flow rate, and r is the radius.

The validity of the Hagen-Poiseuille equation can be examined with the Reynolds number, Re, where if $Re < 2100$, then the flow in the fibre can be considered to be laminar (Lipski and Coˇté, 1990).

A.4. Energy balance equations

There are many pieces of literature reporting the energy balance equations used (Marriott, 2001; Hafrat et al., 2016; Lee et al., 2016; Meng et al., 2020; Babaie and Nasr Esfahany, 2020), and those energy balance equations are also used in this work, where:

$$\frac{dh_{ret}}{dt} = \frac{F_{feed}\,h_{feed} - F_{ret}\,h_{ret} - F_{perm}\,h_{perm}}{M_{ret}} \tag{A12}$$

where h is the specific enthalpy, F is the molar flow rate, and M is the molar holdup.

Under the steady-state condition, Equation (A12) can be simplified to:

$$F_{feed}\,h_{feed} = F_{ret}\,h_{ret} + F_{perm}\,h_{perm} \tag{A13}$$

The specific enthalpy is obtained from Multiflash (KBC Advanced Technologies, 2015), where it is a function of the temperature, pressure, and composition of the retentate side, $h = f(T, P, \mathbf{x})$.

B. Costing equations

This section presents the equations used to calculate the costs of the units (other than for the distillation column, which can be found in Duanmu et al. (2022b) used in this work. The equations for the membrane are taken from González and Ortiz (2002), while the equations for the other units are obtained from Sinnott and Towler (2020). The parameters used in calculating capital, operating, and total annualised costs are shown in Table B1.

In general, the capital cost (CAPEX) and operating cost (OPEX) are used to calculate the total annualised cost (TAC) with the following equation:

$$\text{TAC} = \frac{\text{CAPEX}}{\text{PaybackPeriod}} + \text{OPEX} \tag{B1}$$

where the CAPEX and OPEX take into account all the units and utilities, respectively. The payback period and annual operating hours are assumed to be eight years and $8400\,h\,y^{-1}$, respectively (Duanmu et al., 2022b).

B.1 Membrane

The costs of the pervaporation membrane are taken from González and Ortiz (2002), which are based on the prices in 2007. Therefore, appropriate scaling using the Chemical

Table B1 – Values and references of the parameters used for the calculation of capital, operating, and total annualised costs.			
Items	Values	Units	References
Chemical Engineering Plant Cost Index (CEPCI)			
2002	396	–	Turton et al. (2012)
2007	509.7	–	Sinnott and Towler (2020)
2019	607.5	–	Jenkins (2020)
Equipment Material			
Material	Stainless steel	–	Sinnott and Towler (2020)
Material factor, f_m (stainless steel)	1.3	–	Sinnott and Towler (2020)
Lang Factor, f_{Lang}			
Distillation columns, pumps	4	–	Sinnott and Towler (2020)
Condensers, reboilers, heat exchangers	3.5	–	Sinnott and Towler (2020)
Membranes	3.36	–	González and Ortiz (2002)
Heat Exchanger Sizing Parameter			
Temperature difference, ΔT	10	K	Tsatse et al. (2021)
Heat transfer coefficient, U	0.750	$kW\,m^{-2}\,K^{-1}$	Tsatse et al. (2021)
Utility Costs			
Low pressure (LP) steam	14.05	$\$\,GJ^{-1}$	Turton et al. (2012)
Medium pressure (MP) steam	14.83	$\$\,GJ^{-1}$	Turton et al. (2012)
High pressure (HP) steam	17.70	$\$\,GJ^{-1}$	Turton et al. (2012)
Cooling water, inlet at 30°C	0.354	$\$\,GJ^{-1}$	Turton et al. (2012)
Chilled water, inlet at 5°C	4.43	$\$\,GJ^{-1}$	Turton et al. (2012)
Refrigerant (− 20°C)	7.89	$\$\,GJ^{-1}$	Turton et al. (2012)
Refrigerant (− 50°C)	13.11	$\$\,GJ^{-1}$	Turton et al. (2012)
Electricity	16.8	$\$\,GJ^{-1}$	Turton et al. (2012)

Engineering Plant Cost Index (CEPCI) should be applied. The capital cost (CAPEX) of the membrane can be calculated by (González and Ortiz, 2002):

$$CAPEX_{mem} = f_{Lang}\ Price_{mem}\ A_{tot,mem} \qquad (B2)$$

where f_{Lang} is the Lang factor (see Table B1), $Price_{mem}$ is the price per area of the membrane (see Table 1), and $A_{tot,mem}$ is the total membrane area required.

The membrane replacement cost, which is calculated as part of the operating cost (OPEX), can be calculated from the equation (González and Ortiz, 2002):

$$OPEX_{mem} = \frac{Price_{repl.}\ A_{tot,mem}}{t_{mem}} \qquad (B3)$$

where $Price_{repl.}$ is the membrane replacement cost per area per year (see Table 1) and t_{mem} is the membrane lifetime which is assumed to be two years (González and Ortiz, 2002).

B.2. Heaters and Coolers

The heaters and coolers (including the membrane network heaters) are considered as U-tube shell and tube heat exchangers. The CAPEX of the heat exchanger can then be calculated with (Sinnott and Towler, 2020):

$$CAPEX_{HEX} = f_{Lang}\ f_m\ (24000 + 46\ A_{HEX}^{1.2}) \qquad (B4)$$

where f_{Lang} and f_m are the Lang factor and material factor, respectively (see Table B1), and A_{HEX} (m^2) is the heat exchanger require calculated with (Luyben, 2013):

$$A_{HEX} = \frac{Q_{HEX}}{U\ \Delta T} \qquad (B5)$$

where Q_{HEX} is the heating/cooling duty, and U and ΔT are the heat transfer coefficient and typical temperature difference, respectively (see Table B1).

The operating cost for the heat exchanger (heaters or coolers) can be calculated by:

$$OPEX_{HEX} = Price_{util.}\ Q_{HEX} \qquad (B6)$$

where $Price_{util.}$ is the price of the (heating or cooling) utility used, and the type of the utility is decided automatically by the optimiser depending on the outlet temperatures of the heat exchangers.

B.3. Pumps

The cost equation for the pump is taken from Sinnott and Towler (2020), where:

$$CAPEX_{pump} = f_m\ (6900 + 206\ \dot{V}^{0.9}) \qquad (B7)$$

where f_m is the material factor (see Table B1) and $\dot{V}$ $(L\ s^{-1})$ is the inlet volumetric flow rate.

The operating cost of the pump can be calculated with:

$$OPEX_{pump} = Price_{elec.}\ P_{pump} \qquad (B8)$$

where $Price_{elec.}$ is the price of the electricity (see Table B1) and P_{pump} (kW) is the power required by the pump.

References

Andre, A., Nagy, T., Toth, A.J., Haaz, E., Fozer, D., Tarjani, J.A., Mizsey, P., 2018. Distillation contra pervaporation: comprehensive investigation of isobutanol-water separation. J. Clean. Prod. 187, 804–818.

Babaie, O., Nasr Esfahany, M., 2020. Optimization of a new combined approach to reduce energy consumption in the hybrid reactive distillation-pervaporation process. Chem. Eng. Process. - Process. Intensif. 151 (March), 107910.

Bausa, J., Marquardt, W., 2000. Shortcut design methods for hybrid membrane/distillation processes for the separation of nonideal multicomponent mixtures. Ind. Eng. Chem. Res. 39 (6), 1658–1672.

Chia, D.N., Duanmu, F., Sorensen, E., 2021. Optimal design of distillation columns using a combined optimisation approach. In: Turkay, M., Gani, R. (Eds.), 31st European Symposium on Computer Aided Process Engineering. Elsevier B.V, pp. 153–158.

Chia, D.N., Sorensen, E., 2022. Optimal design of hybrid distillation/ pervaporation processes. In: Yamashita, Y., Kano, M. (Eds.), Proceedings of the 14th International Symposium on Process Systems Engineering - PSE2021+. Elsevier B.V, pp. 313–318.

Deb, K., 2000. An efficient constraint handling method for genetic algorithms. Comput. Methods Appl. Mech. Eng. 186 (2–4), 311–338.

Demirel, S.E., Li, J., Hasan, M.M., 2017. Systematic process intensification using building blocks. Comput. Chem. Eng. 105, 2–38.

Demirel, S.E., Li, J., Hasan, M.M., 2021. Membrane separation process design and intensification. Ind. Eng. Chem. Res. 60 (19), 7197–7217.

Duanmu, F., Chia, D.N., Sorensen, E., 2022a. A combined particle swarm optimization and outer approximation optimization strategy for the optimal design of distillation systems. In: Yamashita, Y., Kano, M. (Eds.), Proceedings of the 14th International Symposium on Process Systems Engineering - PSE2021+. Elsevier B.V, pp. 1315–1320.

Duanmu, F., Chia, D.N., Sorensen, E., 2022b. A shortcut design method for complex distillation structures. Chem. Eng. Res. Des. 180, 346–368.

El-Halwagi, M.M., 1992. Synthesis of reverse-osmosis networks for waste reduction. AIChE J. 38 (8), 1185–1198.

Evangelista, F., 1989. Design and performance of two-stage reverse osmosis plant. Chem. Eng. Process. 25 (3), 119–125.

Fan, L., Cheng, C., Ho, L., Hwang, C., Erickson, L., 1968. Analysis and optimization of a reverse osmosis water purification system Part I. Process analysis and simulation. Desalination 5 (3), 237–265.

Gani, R., Bek-Pedersen, E., 2000. Simple new algorithm for distillation column design. AIChE J. 46 (6), 1271–1274.

González, B., Ortiz, I., 2002. Modelling and simulation of a hybrid process (pervaporation-distillation) for the separation of azeotropic mixtures of alcohol-ether. J. Chem. Technol. Biotechnol. 77 (1), 29–42.

Hafrat, M., Tgarguifa, A., and Abderafi, S. (2016). Modeling of pervaporation process for the dehydration of bioethanol. Proceedings of 2015 IEEE International Renewable and Sustainable Energy Conference, IRSEC 2015, 1–6.

Holtbrugge, J., 2016. Chapter 6: Membrane-assisted (reactive) distillation. In: Lutze, P., Gorak, A. (Eds.), Reactive and Membrane-Assisted Separations. De Gruyter, Berlin, Boston, pp. 237–311 chapter 6.

Jenkins, S. (2020). 2019 Chemical Engineering Plant Cost Index Annual Average.

Kanchanalai, P., Realff, M.J., Kawajiri, Y., 2012. Optimal Process Configurations of Bioethanol Dehydration for Different Ethanol Inlet Concentrations and Throughputs. 31 Elsevier Masson SAS,.

Katoh, T., Tokumura, M., Yoshikawa, H., Kawase, Y., 2011. Dynamic simulation of multicomponent gas separation by hollow-fiber membrane module: nonideal mixing flows in permeate and residue sides using the tanks-in-series model. Sep. Purif. Technol. 76 (3), 362–372.

KBC Advanced Technologies, 2015. Multiflash Version 6.1.

Kimura, S., Sourirajan, S., Ohya, H., 1969. Stagewise reverse osmosis process design. Ind. Eng. Chem. Process Des. Dev. 8 (1), 79–89.

Koch, K., Sudhoff, D., Kreiß, S., Górak, A., Kreis, P., 2013. Optimisation-based design method for membrane-assisted separation processes. Chem. Eng. Process.: Process.Intensif. 67, 2–15.

Kookos, I.K., 2002. A targeting approach to the synthesis of membrane networks for gas separations. J. Membr. Sci. 208 (1–2), 193–202.

Lee, H.-Y., Li, S.-Y., Chen, C.-L., 2016. Evolutional design and control of the equilibrium-limited ethyl acetate process via reactive distillation-pervaporation hybrid configuration. Ind. Eng. Chem. Res. 55 (32), 8802–8817.

Lelkes, Z., Szitkai, Z., Rev, E., Fonyo, Z., 2000. Rigorous MINLP model for ethanol dehydration system. Comput. Chem. Eng. 24 (2–7), 1331–1336.

Li, G., Bai, P., 2012. New operation strategy for separation of ethanol-water by extractive distillation. Ind. Eng. Chem. Res. 51 (6), 2723–2729.

Li, G., Wang, C., Guang, C., Zhang, Z., 2020. Energy-saving investigation of hybrid reactive distillation for n-butyl acetate production from two blending feedstocks. Sep. Purif. Technol. 235 (September 2019), 116163.

Li, H., Guo, C., Guo, H., Yu, C., Li, X., Gao, X., 2019. Methodology for design of vapor permeation membrane-assisted distillation processes for aqueous azeotrope dehydration. J. Membr. Sci. 579 (March), 318–328.

Lipnizki, F., Field, R.W., Ten, P.-K., 1999. Pervaporation-based hybrid process: a review of process design, applications and economics. J. Membr. Sci. 153 (2), 183–210.

Lipski, C., Co̧té, P., 1990. The use of pervaporation for the removal of organic contaminants from water. Environ. Prog. 9 (4), 254–261.

Liu, J., Gao, L., Liu, X., Ren, J., Dong, M., Sun, L., 2022. Evolutional design and plant-wide control for dimethyl ether production by combining dynamic process intensification and pervaporation membranes. Ind. Eng. Chem. Res. 61 (14), 4920–4936.

Luyben, W.L., 2005. Effect of feed composition on the selection of control structures for high-purity binary distillation. Ind. Eng. Chem. Res. 44 (20), 7800–7813.

Luyben, W.L., 2009. Control of a column/pervaporation process for separating the ethanol/water azeotrope. Ind. Eng. Chem. Res. 48 (7), 3484–3495.

Luyben, W.L., 2013. Distillation Design and Control Using Aspen™ Simulation, second ed. John Wiley & Sons, Inc., USA.

Marriott, J. (2001). Detailed Modelling and Optimal Design of Membrane Separation Systems. PhD thesis, University College London.

Marriott, J., Sorensen, E., 2003a. A general approach to modelling membrane modules. Chem. Eng. Sci. 58 (22), 4975–4990.

Marriott, J., Sorensen, E., 2003b. The optimal design of membrane systems. Chem. Eng. Sci. 58 (22), 4991–5004.

Meng, D., Dai, Y., Xu, Y., Wu, Y., Cui, P., Zhu, Z., Ma, Y., Wang, Y., 2020. Energy, economic and environmental evaluations for the separation of ethyl acetate/ethanol/water mixture via distillation and pervaporation unit. Process Saf. Environ. Prot. 140, 14–25.

Micovic, J., Werth, K., Lutze, P., 2014. Hybrid separations combining distillation and organic solvent nanofiltration for separation of wide boiling mixtures. Chem. Eng. Res. Des. 92 (11), 2131–2147.

Naidu, Y., Malik, R.K., 2011. A generalized methodology for optimal configurations of hybrid distillation-pervaporation processes. Chem. Eng. Res. Des. 89 (8), 1348–1361.

Pan, C.Y., 1986. Gas separation by high-flux, asymmetric hollow-fiber membrane. AIChE J. 32 (12), 2020–2027.

Process Systems Enterprise (2021). gPROMS Process version 2.2.

Process Systems Enterprise (2022). gO:Run.

Purkait, M.K., Singh, R., 2018. Membrane Technology in Separation Science. CRC Press.

Roth, T., Kreis, P., Górak, A., 2013. Process analysis and optimisation of hybrid processes for the dehydration of ethanol. Chem. Eng. Res. Des. 91 (7), 1171–1185.

Santoso, A., Yu, C.C., Ward, J.D., 2012. Analysis of local recycle for membrane pervaporation systems. Ind. Eng. Chem. Res. 51 (29), 9790–9802.

Sinnott, R., Towler, G., 2020. Chemical Engineering Design, sixth ed. Elsevier.

Skiborowski, M., Harwardt, A., Marquardt, W., 2013. Conceptual design of distillation-based hybrid separation processes. Annu. Rev. Chem. Biomol. Eng. 4 (1), 45–68.

Skiborowski, M., Wessel, J., Marquardt, W., 2014. Efficient optimization-based design of membrane-assisted distillation processes. Ind. Eng. Chem. Res. 53 (40), 15698–15717.

Szitkai, Z., Lelkes, Z., Rev, E., Fonyo, Z., 2002. Optimization of hybrid ethanol dehydration systems. Chem. Eng. Process.: Process.Intensif. 41 (7), 631–646.

Tgarguifa, A., Abderafi, S., Bounahmidi, T., 2018. Energy efficiency improvement of a bioethanol distillery, by replacing a rectifying column with a pervaporation unit. Renew. Energy 122, 239–250.

Tsatse, A., Oudenhoven, S., tenKate, A., Sorensen, E., 2021. Optimal design and operation of reactive distillation systems based on a superstructure methodology. Chem. Eng. Res. Des. 170, 107–133.

Tsuyumoto, M., Akita, K., Teramoto, A., 1995. Pervaporative transport of aqueous ethanol: dependence of permeation rates on ethanol concentration and permeate side pressures. Desalination 103 (3), 211–222.

Tsuyumoto, M., Teramoto, A., Meares, P., 1997. Dehydration of ethanol on a pilot-plant scale, using a new type of hollow-fiber membrane. J. Membr. Sci. 133 (1), 83–94.

Tula, A.K., Befort, B., Garg, N., Camarda, K.V., Gani, R., 2017. Sustainable process design & analysis of hybrid separations. Comput. Chem. Eng. 105, 96–104.

Tula, A.K., Eden, M.R., Gani, R., 2020. Computer-aided process intensification: challenges, trends and opportunities. AIChE J. 66 (1), 1–12.

Turton, R., Bailie, R., Whiting, W., Shaeiwitz, J., Bhattacharyya, D., 2012. Analysis, Synthesis, and Design of Chemical Processes, fourth ed. Pearson.

Uppaluri, R.V.S., Linke, P., Kokossis, A.C., 2004. Synthesis and optimization of gas permeation membrane networks. Ind. Eng. Chem. Res. 43 (15), 4305–4322.

Valentínyi, N., Mizsey, P., 2014. Comparison of pervaporation models with simulation of hybrid separation processes. Period. Polytech. Chem. Eng. 58 (1), 7.

Van Hoof, V., Van den Abeele, L., Buekenhoudt, A., Dotremont, C., Leysen, R., 2004. Economic comparison between azeotropic distillation and different hybrid systems combining distillation with pervaporation for the dehydration of isopropanol. Sep. Purif. Technol. 37 (1), 33–49.

Vane, L.M., 2013. Pervaporation and vapor permeation tutorial: membrane processes for the selective separation of liquid and vapor mixtures. Sep. Sci. Technol. 48 (3), 429–437.

Wang, C., Wang, C., Guang, C., Gao, J., Zhang, Z., 2019. Hybrid reactive distillation using polyoctylmethylsiloxane membrane for isopentyl acetate production from mixed PVA by products. J. Chem. Technol. Biotechnol. 94 (2), 527–537.

Wu, Y., Meng, D., Yao, D., Liu, X., Xu, Y., Zhu, Z., Wang, Y., Gao, J., 2020. Mechanism analysis, economic optimization, and environmental assessment of hybrid extractive distillation-pervaporation processes for dehydration of n -propanol. ACS Sustain. Chem. Eng. 8 (11), 4561–4571.

Zarca, R., Ortiz, A., Gorri, D., Biegler, L.T., Ortiz, I., 2018. Optimized distillation coupled with state-of-the-art membranes for propylene purification. J. Membr. Sci. 556 (February), 321–328.

Zhao, Q., Chu, X., Li, Y., Yan, M., Wang, X., Zhu, Z., Cui, P., Wang, Y., Wang, C., 2022. Economic, environmental, exergy (3E) analysis and multi-objective genetic algorithm optimization of isopropyl acetate production with hybrid reactive-extractive distillation. Sep. Purif. Technol. 301 (July), 121973.